Lopsided Galaxies

D. Seekles[1]

31 Augustus, 2005

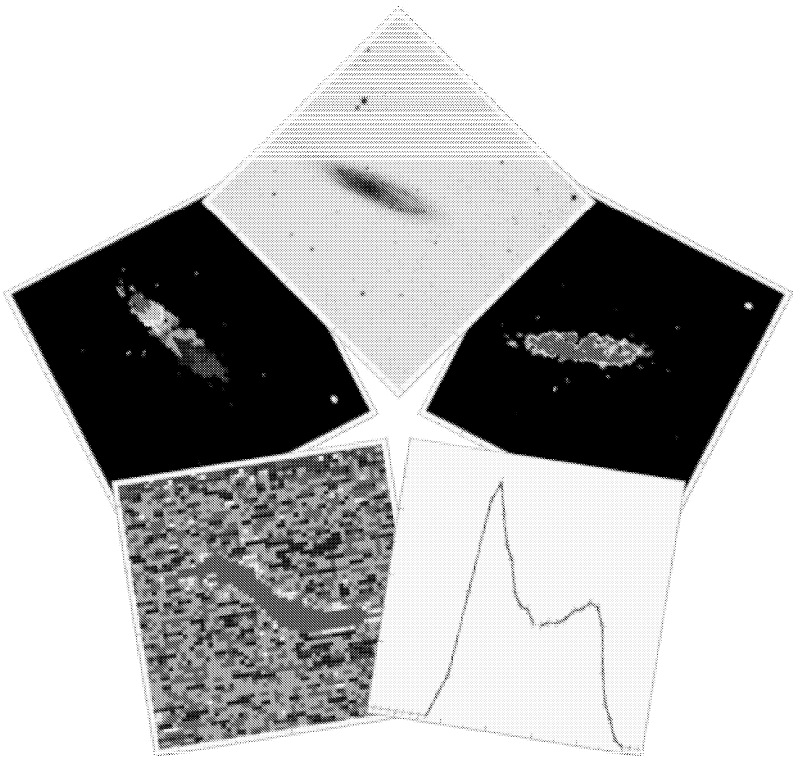

Thesis coordinator : Prof. Dr. J. M. van der Hulst[1].
Main research idea/data provided by : Prof. Dr. R. Sancisi[2]

[1]Rijks Universiteit Groningen, the Netherlands
[2]Osservatorio Astronomico di Bologna, Italy

Contents

List of Figures

List of Tables

The ugly ducklings amongst the fundamental building blocks of the Universe, galaxies, in astronomy are lopsided galaxies. These asymmetric systems cannot match any model appearance of their symmetric counterparts or the sparkling identity of their Arp brothers. But nature always strives for balance and as on Earth the Universe is no less an exception to Mother Nature's whims. Of what is dull and not attractive, their always will be a lot.

In this master thesis I hope to enlighten you on a subject known to exist for over 30 years. Which only in recent years has drawn some theoretical attention but stays in the dark when it comes to a practical analysis of the data present.

D. Seekles

Abstract

Asymmetries in the distribution of light and neutral hydrogen have been known for quite some time. Large scale studies into the occurrence of lopsidedness in the neutral hydrogen , e.g. (Richter and Sancisi, 1994) all have been based on global profiles. The known problem with these global profiles is the possible cancellation of lopsided effects in these profiles. In this Master Thesis we examine the possibility of using the position velocity diagram as a tool to identify lopsidedness in disk galaxies and try to identify from a set of ten strongly lopsided systems key markers for lopsidedness in position velocity diagrams.

Characteristic parameters for 81 symmetric disk galaxies are compared with that of 131 lopsided disk galaxies ranging from type "Sa" to type "Im". This comparison shows no significant difference between the symmetric and the lopsided type of galaxies in these parameters. Also no significant influence of the density distribution of galaxies on lopsidedness is found to exist.

Lopsided galaxies seem to be significantly more often barred then their symmetric counterparts, a factor of 7:5, which might explain why lopsided galaxies often are found to be brighter in L_B then their symmetric counterparts in singular system researches.

1 Introduction

One of the most powerful tools an astronomer has to study the universe and all of it components is the model. Study a sample, preferably statistically as correct as possible, of objects in the universe and from that create a model which all of those objects obey. One then can use this model as a template for study, later on, of other objects, that fall in the same category. But in strength lies weakness. However powerful a model is, is it the truth, does it describe our reality close enough to fit the bill?

Lopsidedness or asymmetry can be one of those cracks in present galaxy models. Recent studies have shown that probably half of all spiral galaxies are lopsided and hence the question arises how accurately symmetric models do represent lopsided spiral galaxies and if not how we should adapt our models to the new situation.

Large scale asymmetries in the optical appearance of spiral galaxies have been known for quite some time (Arp, 1966). Only a few systematic studies have been carried out in the regime though. Baldwin, Lynden-Bell & Sancisi (1980) were the first to draw attention to lopsided HI distributions of spiral galaxies. Their study showed that the lopsidedness is common amongst spiral galaxies and affects the disc as a whole. If lopsidedness does constitute a perturbation on a normal spiral galaxy, where the gas rotates on circular orbits, the lopsidedness would disappear within a few rotational periods, which is about 1 G yr. Baldwin, Lynden-Bell & Sancisi (1980) proposed a model in which the gas moves on initial inclined elliptical orbits in an axisymmetric potential. The lifetime for lopsidedness due to this model is increased considerably to between 1 and 5 G yr, the lopsidedness will however disappear due to differential rotation.

A study of global profiles by Richter & Sancisi (1994) and Haynes et al. (1998), of approximately 1700 HI profiles of spiral galaxies and of 104 HI profiles of isolated spiral galaxies, show that more then 50% of the spiral galaxies is significantly lopsided. However, as mentioned in both articles, the global profile is build up out of two components, the disk kinematics and HI distribution which can cancel each others influence on the global profile and hence the 50% is a lower limit for the amount of lopsided galaxies they found. Richter & Sancis (1994) also confirm the finding from Baldwin, Lynden-Bell & Sancisi (1980) that lopsidedness is a large-scale structural effect affecting the whole disk.

HI profiles of a group of 30 extreme late-type spiral galaxies were studied by Matthews, Van Driel & Gallagher (1998a). They concluded that about 75% of the profiles examined pointed towards the examined spiral galaxies being lopsided and hence they inferred that lopsidedness is more common among late-type spiral galaxies. Swaters (1999) studied a group of 75 late-type spiral

galaxies in Hl and red light. In both the kinematics and the Hl distribution a high incidence of lopsidedness was found. In Swaters et al. (1999) two of the studied galaxies are highlighted. UGC 731 and UGC 7524, also present in the sample studied in this paper, are of type Im and Sm and show lopsidedness in their kinematics but not in their HI distribution or optical appearance and have no nearby companions.

The optical appearance of spiral galaxies and the incidence of lopsidedness has also been studied in a quantitative way. Rix & Zaritsky (1995) studied K-band images of 18 spiral galaxies. Zaritsky & Rix (1997) studied I-band images of 60 galaxies. The incidence, of significant lopsidedness, found in the samples is about one-third. They argue that this number should be lower then the incidence of HI distribution lopsidedness due to the longer dynamical timescales in the outer regions of disks. Their derived wind up time is about 1 G yr. They estimate from their observations of the frequency of occurrence of lopsidedness however that it should be around 3 G yr. They also find that lopsided galaxies have a B-band excess when compared to the B-band luminosity prediction by the Tully-Fisher relation. A study of the optical appearance of the early type S0 to Sab galaxies by Rudnick & Rix (1998) yielded a percentage of 20 for the incidence of optical lopsidedness in their sample.

Lopsidedness in the HI distribution and in the kinematics of spiral galaxies have been studied by Kornreich et al. (2000) (2001) in two papers. In both papers they studied 9 spiral galaxies and found no correlation between the parameters they measured. They draw the conclusion from their findings that "normal morphology is not an indicator of normal kinematics and, conversely, that perturbed kinematics do not necessarily manifest as perturbed optical morphology". In Swaters (1999), (Chapter 3, table A2), the type and strength of the lopsidedness of the studied systems are given. This table shows clearly that lopsidedness in the kinematics does not mean that there is lopsidedness in the HI distribution and vice versa. An interesting point worth noting is that some systems(for example UGC 2053, UGC 3698) have a global profile that hints at lopsidedness, but no trace for lopsidedness is found in either the kinematics or HI distribution of those galaxies. Other examples can be found in Sancisi & Allen (1979) who studied NGC 891 which is lopsided in the HI distribution but displays almost perfect symmetric kinematics, Swaters et al. (1999), as mentioned above, study DDO 9 and NGC 4395 and find lopsided kinematics but no lopsided light or Hl distribution.

The incidence of lopsidedness amongst spiral galaxies is large enough to consider it not being a transient effect but a more permanent feature or at least a general feature. Since the lopsidedness is not a localized irregularity but is affecting the disk of the spiral galaxy as a whole, models need to be found to explain the lopsidedness in a satisfactory way. Most authors on the subject of lopsidedness have come up with a model to explain the lopsidedness

or at least the timescales of the persistence of the found lopsidedness. Over the years these models got more sophisticated with the introduction of fast computers and the possibility of particle simulations. Also advances were made on the analytic front of galaxy modeling.

Baldwin, Lynden-Bell & Sancisi (1980), as mentioned previously, introduced a model that instead of the circular orbits found in 'normal' galaxies used initially aligned elliptical orbits in an axisymmetric potential. Due to differential rotation the lopsidedness in this model will disappear in about 5 G yr. The drawback to this model is that due to the model conserving angular momentum the rotation curve on the 'normal' part of the disk must be considerably higher then on the 'lopsided' part of the disk. The authors also note that they think 5 G yr is not a long enough lifetime for lopsidedness. Zaritsky & Rix (1997) propose a model that uses accretion of small companion galaxies. Using results of N-body simulations by Walker, Mihos & Hernquist (1996) they find that present day lopsidedness can be explained by the accretion of one companion galaxy in the last G yr, this lifetime combined with the frequency of lopsidedness gives them a upper limit on the accretion rate. This accretion rate can be lower if other effects make the lifetime of the lopsidedness more longeval. Rix & Zaritsky (1995) propose a lopsided potential as the solution.

Weinberg (1991), (1994) and later Vesperinin & Weinberg (2000) introduce the use of lopsided modes of oscillation in a spherical system, which they show have very long decay times. When used on galactic halo's the created perturbation will be very long lived. Jog (1997) showed that a perturbation, even a small one, of the galaxy halo can cause strong lopsidedness in the density of disc gas. In a follow up paper, Jog (1999) showed that the gravity of the disc opposes the lopsidedness created in the galaxy's halo, which he already suggested in his previous paper. The lopsidedness that results from this perturbation in the galactic halo is most prominent in the outer parts of the disc, this coincides quite well with the observed form of lopsidedness in galaxies. In the model the dynamical dominance of the galactic halo in the outer parts of the galaxy is responsible for the lopsidedness being more prominent there. Another model including the galactic halo is that of Levine & Sparke (1998) where the galaxy is placed off-center from the galactic halo. N-body simulations by Levine & Sparke (1998) show that, for this model, when a galaxy performs a retrograde rotation compared to the motion around the galaxy halo center, the galaxy can stay off-center for quite a few rotational periods and perform near circular motion at the halo's core radius. A disk that performs prograde rotation compared to the motion around the galactic halo will slowly fall towards the galactic halo's core. Hence lopsidedness will only be able to persist for longer periods in retrograde moving galaxies. No mention is made about the statistics for occurrences of the situation of this model. Noordermeer, Sparke & Levine (2001) use the model of Levine & Sparke (1998) to investigate the kinematics of the gas in such a model. It is

shown that the model can describe the types of possible lopsided combinations in a galaxy quite accurately. As an example NGC 4395(UGC 7524) is used. Lopsidedness in the gas of the model used is the strongest if the halo is more dominant and the conclusion is drawn that this might explain why late-type systems are more often lopsided in their gas distribution then earlier type systems.

Schoenmakers, Franx & de Zeeuw (1997) studied small deviations from axisymmetry of the potential of a filled gas disc. They find that certain harmonic components point toward a certain type of lopsidedness in the disc and that the effects of the perturbation should be visible in the residual velocity fields. Swaters (1999) shows that with use of the formulas presented in the paper of Schoenmakers, Franx & de Zeeuw (1997) model velocity fields can be created. Also it is shown that the shape of the model velocity field depends on the viewing angle.

Data as presented in samples such as that of Richter & Sancisi (Richter and Sancisi, 1994) is of insufficient resolution to examine the detailed properties of lopsided galaxies. To discriminate between the effects of kinematical lopsidedness and morphological lopsidedness high spatial resolution data is required. This type of high resolution data is available in the WHISP database. In this thesis the WHISP database will be used to contruct a lopsided sample of galaxies and a control sample of galaxies in order to find keys toward the origin of lopsidedness.

In chapter 2 we describe the selection of a lopsided sample and control sample also we describe in detail 10 of the most distinctly strong lopsided galaxies, selected from the lopsided sample. In chapter 3 a comparison is made between the properties of the lopsided and control sample. In chapter 4 we focus on the construction and analisys of a new lopsided and control sample based on a set of objective criteria. Conclusions are presented in chapter 5.

2 Data

This section will outline the creation of a lopsided and control sample based on systems present in the WHISP database and on systems present in four PhD. Theses. The lopsided sample will contain a set of weakly lopsided systems and a set of strongly lopsided systems, the data for this sample will mainly be based on data present in the four PhD. Theses. The control sample will contain systems which are selected from the WHISP database on the basis of the selection criteria presented in Richter & Sancisi (1994). From the lopsided sample a set of 10 clear-cut cases of strong lopsidedness are selected to present the reader with an overview of the effect of lopsidedness on the position velocity diagram and velocity field.

2.1 Sources

The sources for the data used in this project are retrieved from a number of databases and PhD. Theses. The position-velocity diagrams and velocity fields studied in 2.3.1 on page 15 are retrieved from the WHISP(Westerbork observations of neutral Hydrogen in Irregular and SPiral galaxies) database. (van der Hulst et al., 2001)

http://www.astro.rug.nl/∼whisp/

And from Verheijen(1997) for UGC 6745, Broeils(1992) for UGC 6955 and Rhee(1996) for UGC 11651.

The data presented in table 9, table 12 and table 11 is retrieved from the Lyon-Meudon ExtraGalactic Database(LEDA).

http://leda.univ-lyon1.fr/

Other data sources that were used for retrieving parameters for this thesis are: Broeils (1992), Rhee (1996), Swaters (1999), Verheijen (1997) and Tully (1988).

The Groningen Image Processing System(GIPSY) is used to modify and present the position-velocity diagrams and velocity fields in this thesis.

http://www.astro.rug.nl/∼gipsy/

There are a number of problems that arise when different databases are used to build up a sample of systems that are going to be studied. First of all some astronomical databases, like for example LEDA are subject to regular updates. Not only of the data present but sometimes even the way their parameters are represented. Therefore the reader should be aware that checking the values used in this master thesis could lead to differences when compared to presently available numbers in the databases. Secondly errors can not always be

retrieved from either the used databases or the used PhD. Thesis. Thirdly there is the problem of uniformity of the data within the sample. To avoid the risk of comparing the figurative apple and orange in some cases the choice will be made to use less accurate data which is available for all the systems, instead of higher accuracy data(comparison of accuracy is based on errors found in both sources) which is fragmented between databases and PhD. Thesis. This choice will only be made if it is either impossible to convert data from one source to another or it is deemed to time consuming.

2.2 Initial dataset - Lopsided sample

The initial dataset is based on a sample selected by Prof. Dr. R. Sancisi, by eye, from the WHISP database, see van der Hulst et al.(2001), Swaters (1999), Broeils (1992), Rhee (1996) and Verheijen (1997). This set contains fifty systems selected exclusively on the basis of their lopsidedness in the velocity field and position-velocity diagrams. The fifty selected systems were divided up into a group of strong lopsided systems and a group of mild/uncertain lopsided systems.

Of the fifty systems in the selection six systems are twice present. Of these 6 systems UGC 5316 and UGC 11300 are doubly identified, once by their NGC number once by their UGC number. In both thesis and WHISP database these two systems are classified as weakly lopsided. The other four systems(UGC 1888, UGC 4806, UGC 6869 and UGC 11651) however are once classified as strongly lopsided and once classified as weakly lopsided. Of these, two systems, UGC 4806 and UGC 6869, are as the two systems mentioned previously picked out once by their NGC number and once by their UGC number. The other two systems, UGC 1888 and UGC 11651, are from the same thesis(Rhee, 1996) and are both times identified by their NGC number. The reason for the difference in their identification is not known but it serves to show that identifying by eye has it limits. To prevent the possible confusion of the NGC and UGC numbering of the systems the UGC numbering is adopted as the standard for this thesis.
The author of this master thesis identified the 44 systems in Sancisi's list anew. The classification of strong or weak lopsidedness is based on the velocity field, morphology(HI fields), global profile and position-velocity diagrams. This reclassification was done with the intent to update the list in the case new and improved data had become available in the WHISP database and to act as a review method for the classification scheme used.

This classification scheme(both the author's and of Sancisi's) is based on pre selection by eye and hence independent selection decreases the risk of selecting systems that are not meeting the set requirements of being lopsided based on the data present. The reclassification compared to the old one can be found in table 1. The data(figures) used for the classifications can be found in the

WHISP database.

The criteria used to identify lopsidedness are for the global profile as described in the article by Richter & Sancisi (1994), however an estimate by eye is used. A difference of 20% in peak flux difference, a width difference of around 50 km s^{-1} and a total flux difference between the low and high velocity halves of about 40:60 percent. This last criteria has been broadened in range to be usable when studying a global profile without advanced computational tools. Hence applying this third criterion is done with the utmost care and consideration.

For the position-velocity diagrams a comparison between the negative and positive velocity halves is made. The two main criteria are a difference in steepness in the outer and inner parts between the two sides. Also the difference in minimum and maximum velocities, HI gas radius and profile width are taken into account. In the velocity field the curvature of the iso-velocity contours is compared between the approaching and receding side of the field. In the HI-fields the general distribution of the gas is checked to be uniform based on the sides determined from the velocity field.

After classification by the author it became apparent that there were a number of differences, of the 45[3] reviewed systems only 18 systems were put in the same class. This led to a review of all 45 galaxies present in the list by Sancisi and the author together[4] and a combined decision on the classification for the 45 systems is given in table 1. This new list is the one used in this master thesis. The results of this discussion can be found in table 1 in the Sa./Au. column.
The more extreme changes, with respect to Sancisi's list, are explained in table 2.

The final list of systems contains 23 strongly lopsided systems and 14 weakly lopsided systems. These systems together will form a lopsided sample in chapter 3 of this thesis. To get a better idea of the systems in the lopsided sample we will examine a set of 10 systems present in the lopsided sample. The 10 systems that will be selected are strongly lopsided. The reason for this selection criteria is that we expect that trends specific to lopsided systems will show more strongly in more extreme systems.

2.3 Strongly lopsided systems

For the selection of the ten strongly lopsided systems table 1 is used. The decission was made that the systems that were classified strongly lopsided by

[3]The 45^{th} system, UGC 7081, was added by the author when he stumbled on it fiddling with GIPSY and a few test galaxies amongst them UGC 7081

[4]This discussion took place in the presence of Prof. Dr. J. M. van der Hulst, the author's thesis coordinator

Galaxy	San.	Aut.	Sa./Au.	Galaxy	San.	Aut.	Sa./Au.
UGC 731	S	S	S	UGC 6745	S	S	S
UGC 1249	S	N	N	UGC 6833	W	W/N	N
UGC 1501	W	N	N	UGC 6869	S/W	S/U	U
UGC 1888	S/W	S	S	UGC 6955	S	S	S
UGC 3137	S	S	S	UGC 7030	S	W/N	S
UGC 4278	W	W	W	UGC 7075	W	W/U	W
UGC 4499	W	W/N	W	UGC 7081	-	S	S
UGC 4806	S/W	N	N	UGC 7090	S	S	S
UGC 5251	W	S	S	UGC 7151	W	S	S
UGC 5316	W	S/N	S	UGC 7222	W	W	W
UGC 5414	W	S/W	W	UGC 7323	S	S	S
UGC 5446	W	N	N	UGC 7524	S	S	S
UGC 5452	W	W	W	UGC 7766	S	S/U	S
UGC 5459	S	S	S	UGC 9119	W	W	W
UGC 5589	W	S	S	UGC 10310	W	W	W
UGC 5721	W	N	W	UGC 10359	S	S	S
UGC 5786	W	W/N	W	UGC 11300	W	S	S
UGC 5789	S	S	S	UGC 11651	S/W	S	S
UGC 5986	S	S/N	S	UGC 11707	W	S	S
UGC 6161	W	W/N	W	UGC 11891	S	S	S
UGC 6251	W	U	N	UGC 12632	W	W	W
UGC 6446	W	N	N	UGC 12732	W	W/N	W
UGC 6667	W	W	W				

Table 1: Listing of Sancisi's(San.), Author's(Aut.) and combined(Sa./Au.) classification per galaxy. 'S' = strongly lopsided, 'W' = weakly lopsided, 'N' = not lopsided or data not suitable for classification and 'U' = Uncertain. The four 'S/W' classifications in the 'San.' column are the four double classified galaxies. Double classification in the 'Aut.' column means a doubt between the two possibilities based on the data available.

both Prof. Dr. R. Sancisi and the author of this thesis independently should be most suitable for this endeavour. There are eleven such systems present in table 1. After studying the data available for the eleven systems, Prof. Dr. R. Sancisi and the author with cooperation of Prof. Dr. J. M. van der Hulst decided that two of this eleven systems, UGC 5789 and UGC 7323, were not suited for a study into the general characteristics of lopsided systems. UGC 5789 due to a discontinuety in its global profile and UGC 7232 due to an unuseable position velocity diagram. To again complete the sample, UGC 11651 was added.

For each of the ten systems a number of (physical) parameters are retrieved. These parameters are presented, per system, in table 3. The databases from which each parameter is retrieved are presented in table 4. Next to the retrieval of a set of (physical) parameters each systems general properties and

UGC 1249	Member of a pair of galaxies, due to tidal interactions with neighbour UGC 1256 heavy distortions make classification impossible.
UGC 1501	Only the global profile supports the idea of lopsidedness which is not conclusive enough to classify the strength of the lopsidedness.
UGC 4806	Data is inconclusive. UGC 4806 also has a possible companion([GSK2002] 090643.2+332052), which could make it a good candidate for further study if higher resolution data could be gathered.
UGC 5446	Low resolution data makes a conclusive classification impossible.
UGC 6251	Low resolution data makes a conclusive classification impossible.
UGC 6446	The high velocity half in the position-velocity diagram has two extensions that point toward lopsidedness. The strength of these extensions however heavily depends on the visualization chosen. Therefor they are considered artefacts and the system which is by itself symmetric is classified not lopsided.
UGC 6833	Position-velocity field and velocity field show no traces of lopsidedness, the global profile and HI field do. Hence this system is morphologically lopsided. Sancisi list didn't take this into account and hence the system will not be classified lopsided.
UGC 6869	A large warp present in this galaxy makes a classification uncertain.
UGC 12732	Velocity field shows no signs of lopsidedness, global profile and position-velocity diagram point toward a weakly lopsided system and the HI field points towards a strongly lopsided system. Sancisi didn't take into account morphological lopsidedness when classifying the strength of the lopsidedness. Therefor the system is classified weakly lopsided.

Table 2: Reasons for the change in lopsidedness classifications for a number of systems mentioned in table 1

the characteristics of the lopsidedness are discussed per system. Per system a figure with a position velocity diagram and a velocity field will be presented, excepting UGC 11651 for which no velocity field could be retrieved or reproduced and hence only the position velocity diagram will be presented.

To be able to visualize how lopsidedness shows in position velocity diagrams a set of two contours is plotted in the diagram. This contours are created with the help of GIPSY. The contours are mirrored with respect to the center of the diagram to easily be able to compare the differences between the high and low velocity halves in the position velocity diagram.

System	UGC 731	UGC 3137	UGC 5459	UGC 6745	UGC 6955
Type	Im	Sbc*	Sc	Sc (P)	SBm* (P)
Maj. Axis(R)	4.15	4.72			4.2
Optical size Maj. Axis(B)	2.57	2.6	3.3	4.01	4.18
(arcmin) Min. Axis(R)	2.05	1.09			2.09
Min. Axis(B)	1.27	0.60	0.67	1.03	2.08
$\epsilon = (1 - d/D)$	0.506	0.768	0.798	0.744	0.503
r-mag.	12.89	12.61		9.88	
b-mag.	13.74	14.38	11.98	11.06	12.68
R-mag.	-17.47	-18.65		-21.27	
B-mag.	-16.62	-16.88	-19.56	-20.09	-18.68
Distance(pc)	1.18E+07	1.79E+07	2.03E+07	1.70E+07	1.87E+07
$\rho(GalaxiesMpc^3)$	1.30E-01	1.00E-01	2.70E-01	1.53E+00	3.80E-01
Log of M_{HI}/M_T (Msun)	9.12/-	9.53/10.30	9.67/10.45	9.23/10.72	9.44/10.20
Group membership	17 -2	12+11	13 -1	12 -1	12 +6 +1
Companion(s)	No	No	No	Possible	Possible

System	UGC 7090	UGC 7524	UGC 10359	UGC 11651	UGC 11891
Type	S(B)c (P)	Sm	SBc*	Scd	Im
Maj. Axis(R)		14.45			
Optical size Maj. Axis(B)	5.01	12.02	4.9	2.85	4.07
(arcmin) Min. Axis(R)		9.13			
Min. Axis(B)	1.56	7.60	3.96	0.51	3.14
$\epsilon = (1 - d/D)$	0.689	0.368	0.192	0.821	0.227
r-mag.		9.58			
b-mag.	10.17	10.79	11.85	13.37	13.63
R-mag.		-18.20			
B-mag.	-19.55	-16.99	-19.50	-18.50	-16.48
Distance(pc)	8.80E+06	3.60E+06	1.86E+07	2.37E+07	1.05E+07
$\rho(GalaxiesMpc^3)$	4.00E-01	4.00E-01	1.20E-01	6.00E-02	7.00E-02
Log of M_{HI}/M_T (Msun)	9.12/10.52	9.19/10.07	9.99/10.90	9.44/10.60	9.40/10.15
Group membership	14 -4	14 -7	44 -0 +1	64 -0	65 -0
Companion(s)	No	No	Possible	No	Possible

Table 3: Ten strong lopsided systems parameter overview

Type	:	The morphological type has been determined by comparing the type from WHISP, UGC "catalogue"(Nilson, 1973) and NGC "catalogue"(Tully, 1988) and if the system is present in a PhD. Th. that determination is given precedence. Differences are most often restricted to 1 full classification, when larger errors were present a new morphological type was determined by eye from the optical data.
Optical size	:	In both the R-band(R) and B-band(B) the data are taken from the PhD. Th. if not present the data is taken from LEDA. Brent Tully's NGC values are ignored since a number of them show large differences with for example Swaters (1999) who has data of a much higher quality.
Ellipticity(ϵ)	:	ϵ or $(1 - d/D)$ is taken directly from the PhD. Th.. If the inclination is available that will be transformed into ϵ. If more inclinations are available an average is used to calculate ϵ. If no PhD. Th. contains the system the inclination from LEDA is used to calculate ϵ.
Magnitudes	:	The PhD. Th. are given preference over the databases. If the data is not available in the PhD. Th. it is taken from LEDA. The data from LEDA is corrected for the H0 of 70 that is used to the 75 that is used in the articles. For calculations from absolute to apparent the distance in the PhD. Th. is used.
Distance	:	For reasons of uniformity the distance is taken from Brent Tully's NGC. This distances can't be used to transform the magnitudes columns.
Density(ρ)	:	Taken from Brent Tully's NGC.
HI-mass	:	Taken from WHISP.
Group membership	:	Taken from Brent Tully's NGC.
Companion(s)	:	The SIMBAD database is used to search for companions as was the NGC catalogue, in SIMBAD the standard 10 arcmin is replaced by assuming a search radius based on the distance and a perpendicular velocity on the line-of-sight velocity of 300 km s^{-1}, next to using a 1 G yr timelimit. This time limiis based on the average accretion rate determined by Zaritsky & Rix (1997). Also articles present in NED were scanned for information on possible companions.

Table 4: List of sources used for retrieving the parameters for the systems in the tables, listed per parameter.

To be able to mirror the contours the center of the position velocity diagram needs to be determined. Determining this center is complicated by the systems we study being lopsided. Assymmetries in the neutral hydrogen gas

distribution and the kinematics of the neutral hydrogen gas can cause the center to be off-center from $v_{sys} = 0$ km s^{-1} as well as the center of the major axis. There is no solid solution for this problem as the magnitude of the offset is not known, not even if there is an offset. However we are studying kinematical lopsidedness in the neutral hydrogen gas. The advantage of this type of lopsidedness is that we know it appears most strongly in the outer parts of the disc and hence in the position velocity diagram it will also show there most prominently[5] Another advantage is that the effect of lopsidedness in the inner parts of a position velocity diagram mainly shows in a difference in slope between the two velocity halves, details are most often lost for the center in position velocity diagrams. Hence a slight offset in the rotation of the contours will not effect the difference in the slopes for the inner parts and hence the chances to detect lopsidedness. With this in mind the center for the mirroring is determined in three steps. First the contours are rotated 180 degrees. Secondly the center based on the maximum and minimum velocity and offset on the major axis are determined to find the approximate location of the center. Thirdly the inner, rotated, contours are fitted to the inner parts of the position velocity diagram. In the case of symmetric systems step two would have determined the "exact" center of the system.

For three systems, UGC 6745, UGC 6955 and UGC 11651 there is no WHISP data available and also it was impossible to retrieve the data used in the study of this systems. Therefor the given centers were adopted from the PhD. Thesis the systems originate from and used as the mirroring centers for the contours.

The colour scheme used for the position velocity diagrams and the velocity fields is the so called RonEkers scheme. This scheme uses a maximum of 9 colours to represent the data in a series of discrete bins, next to a fixed center value which the user defines. It is particularly usefull when studying large scale differences since the used colour scheme emphasizes these differences. For the position velocity diagrams the center value will be fixed at a signal-to-noise level of 0 for which we choose the transition from the bin defined by the light blue colour to that of the dark green colour as in accordance to general practise. The bin width is chosen to be 1 σ, where per system this σ is expressed in Westerbork Units or units of 5 mJy/Beam. For the velocity fields the data is represented in 8 bins, ranging from red for the receding side to purple for the approaching side. The center value for the velocity fields is $v_{sys} = 0$ km s^{-1} at the transition off the dark green to the light green bin. The threshold for the signal-to-noise level for the velocity fields is 3σ, excluding UGC 6745 and UGC 6955 for which the cut-off in σ levels is unknown and UGC 11651 for which no velocity field is present, signal that does not meet this threshold is removed and is denoted by the black coloured regions.
The center for the velocity fields does not necessarily have to correspond with

[5]The inner regions of the HI disk lie within the stellar disk of the system, most often making up over 80 percent of the total mass, and it is assumed they suffer from a large dampening effect.

the velocity center of the position-velocity diagram.

2.3.1 The systems

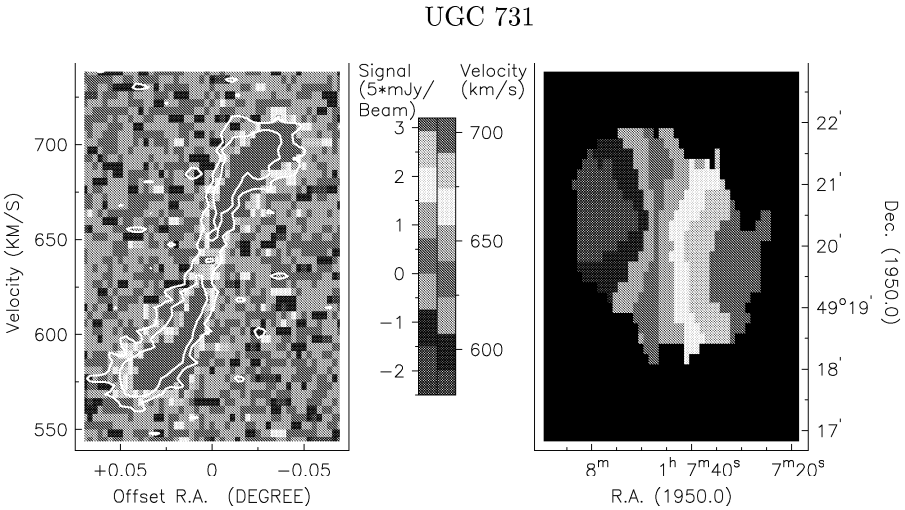

Figure 1: UGC 731

The 1 σ level for the position velocity diagram of UGC 731 is 0.708 Westerbork Units(5mJy/Be). The contours plotted in the position velocity diagram show the 2 σ and 5 σ level. The inclination of the system is 73 degrees.

UGC 731's position-velocity diagram is a good example of what a classical lopsidedness should look like. The slope of the diagram rises more steeply on the left hand side then the right hand side. Also the turnover is more abrupt on the left hand side then the right hand side. The left hand side shows a clear flattening out while on the right hand side it is not fully clear what happens. It seems a slight rising trend is present but due to the absence of gas further out it is not possible to confirm this trend. However the difference in steepness of the slopes also confirms the presence of lopsidedness.

The velocity field supports that the system UGC 731 is lopsided by showing clearly distinct curvature of the different velocity regions on both sides of the system. The curvature of the regions in the blue side are greater then the curvature of the red side of the system.

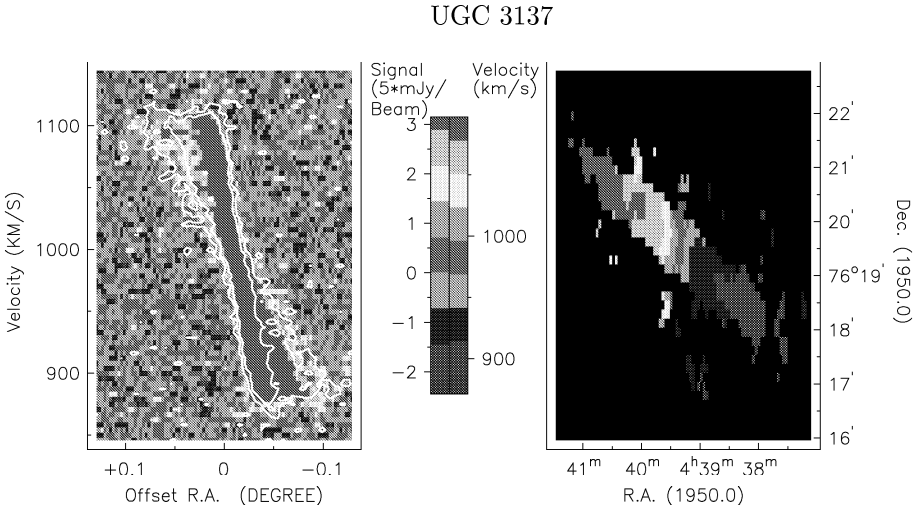

Figure 2: UGC 3137

The 1 σ level for the position velocity diagram of UGC 3137 is 0.723 Westerbork Units. The contours plotted in the position velocity diagram show the 2 σ and 5 σ level. The inclination of the system is 88 degrees.

UGC 3137's position-velocity field is one of the best examples of how one can modify a position-velocity field appearance to highlight lopsidedness. If one would look at the field that is present on the homepage of the WHISP project one would not doubt to call the system strongly lopsided. In the modified figure used here the signs for lopsidedness are much harder to detect. The center part of the diagram doesn't show a noticeable difference between the two sides. The turn over is different but this becomes only clear when one overlays the contours. The right side turnover is more abrupt then that of the left side. Clearest lopsided feature is the flat outer right part compared to the decreasing slope in the outer left part. This is again best seen by using the overlaid contours. Also it can be clearly seen that in the outer parts there is gas present in the right hand side of the diagram where it is not on the left hand side. Though this is due to lopsidedness in the HI which lies outside the scope of this article.

The velocity field of UGC 3137 is not usable to support the findings in the position-velocity diagram it being to highly inclined.

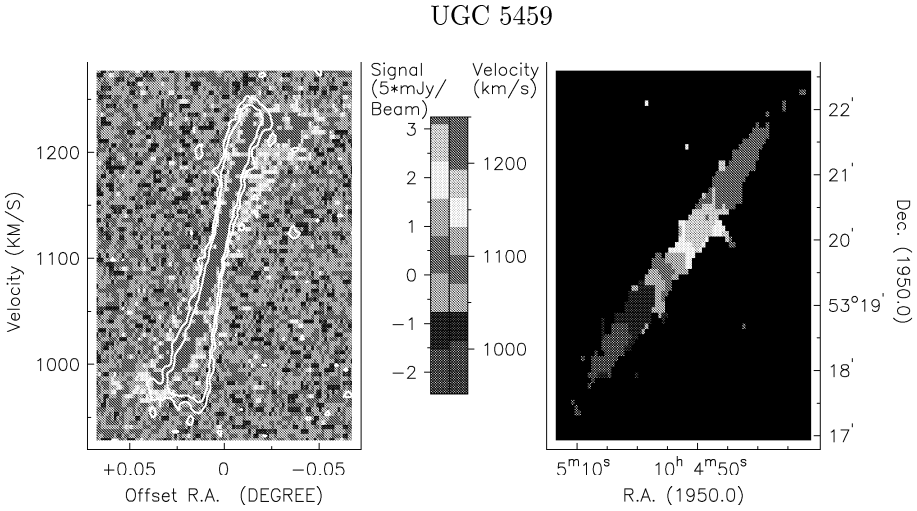

Figure 3: UGC 5459

The 1 σ level for the position velocity diagram of UGC 5459 is 0.765 Westerbork Units. The contours plotted in the position velocity diagram show the 2 σ and 5 σ level. The inclination of the system is 90 degrees.

UGC 5459's position-velocity field is a good example of the points needed to identify lopsidedness. In the inner parts of the diagram there is a difference between the slopes though not as apparent on the outside as on the inside. There is an abrupt turn of on one side compared to the other side, right and left. The outer parts of the diagram show a declining right side and increasing left side. However the bad signal to noise ratio makes it hard to judge if there is any chance of missed gas on the outer sides which could influence the angle of the slope.

UGC 5459's velocity field is edge on and of low data quality, there is a slight hint towards less curvature in the approaching side then the receding side. However the data is of too poor quality to be used conclusively.

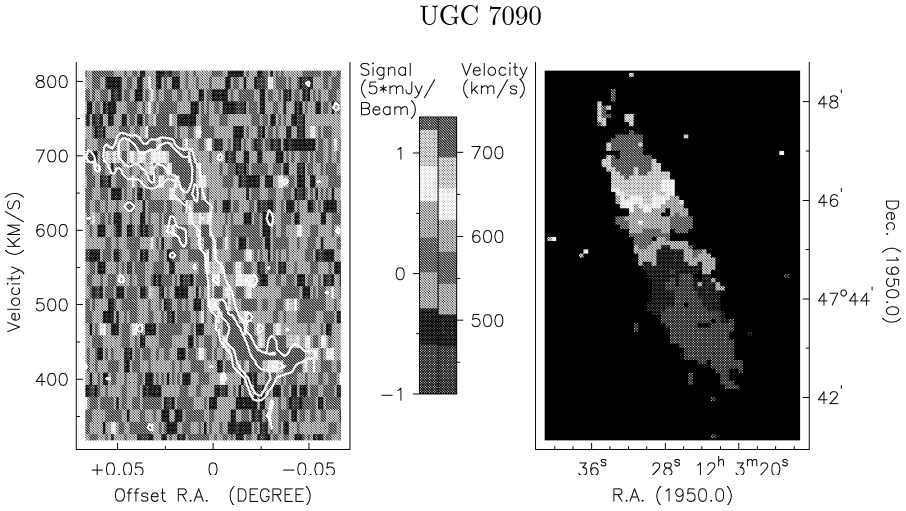

Figure 4: UGC 7090

The 1 σ level for the position velocity diagram of UGC 7090 is 0.304 Westerbork Units. The contours plotted in the position velocity diagram show the 2 σ and 5 σ level. The inclination of the system is 76 degrees.

UGC 7090 suffers from low signal levels which causes a quite unsmooth representation. The use of contours however allows for identification of lopsidedness. The inner contour slopes are steeper on the right side then the left side. The turnoff is much more abrupt, almost 90 degrees on the right side compared to the left side. Also the contours are flat on the left outside part and clearly have a positive slope on the right side. UGC 7090's velocity field isovelocity lines have a higher degree of curvature on the receding side then the approaching side of the system, supporting the lopsidedness found in the position-velocity diagram.

Note: This galaxy seems to have a huge pizza-like slice taken out in the optical data and in the HI on the approaching side there is also clearly HI missing. This is however in no way represented in the position-velocity diagram which is intriguing.

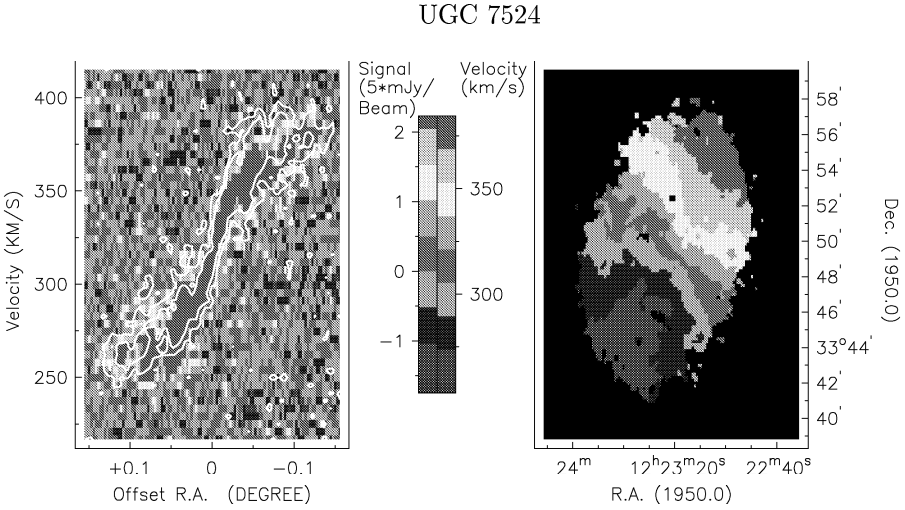

Figure 5: UGC 7524

The 1 σ level for the position velocity diagram of UGC 7524 is 0.515 Westerbork Units. The contours plotted in the position velocity diagram show the 2 σ and 5 σ level. The inclination of the system is 58 degrees.

UGC 7524's position-velocity diagram inner region is somewhat harder to judge then the higher inclination systems we showed. Due to the inclination being low there is a much smaller difference between the minimum and maximum velocity present in the system. This has as consequence that differences between the approaching and receding side of a system can be suppressed and hard to spot by eye. This is the case for UGC 7524. Also there is no strong turnover from inner to outer region of the system present when one compares both sides of the diagram. The outer parts of the system however show the distinctive sign of a rising slope on the right and a flat even slowly decreasing slope on the left of the diagram. UGC 7524's velocity diagram is a prime example of how lopsidedness changes a velocity diagram appearance if the system is viewed under the right position angle. The curvature in velocity field of the receding side is almost absent while the curvature of the approaching side is almost parabolic.

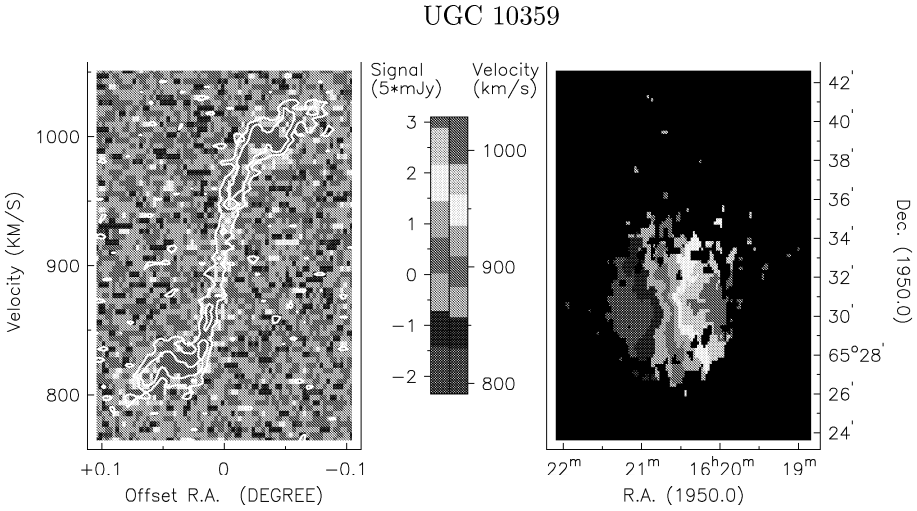

Figure 6: UGC 10359

The 1 σ level for the position velocity diagram of UGC 10359 is 0.718 Westerbork Units. The contours plotted in the position velocity diagram show the 2 σ and 5 σ level. The inclination of the system is 37 degrees.

UGC 10359's position-velocity field has the same problems as the field of UGC 7524, due to low inclination. It is not as apparent in this case since a small offset(x-axis deviation) counters the effect somewhat. The approaching side of the diagram seems to be built up out of three parts, this is however best seen when comparing the contours of the approaching side with the colour scheme levels of the receding side. The innermost region does not match, the contours have a steeper slope then the red part of the diagram which they should match. Than both contours and red diagram part overlap to a high degree after a small turnover in the contours. The third part shows the contours following an increasing slope while the red part of the diagram flattens out after their turnover.

UGC 10359's velocity field resembles that of UGC 7524 quite remarkably though here there is a bit more noise present and the curvature difference is flipped between receding and approaching side. The red velocity part almost has a 90 degree angle compared the the extremely flat purple velocity part.

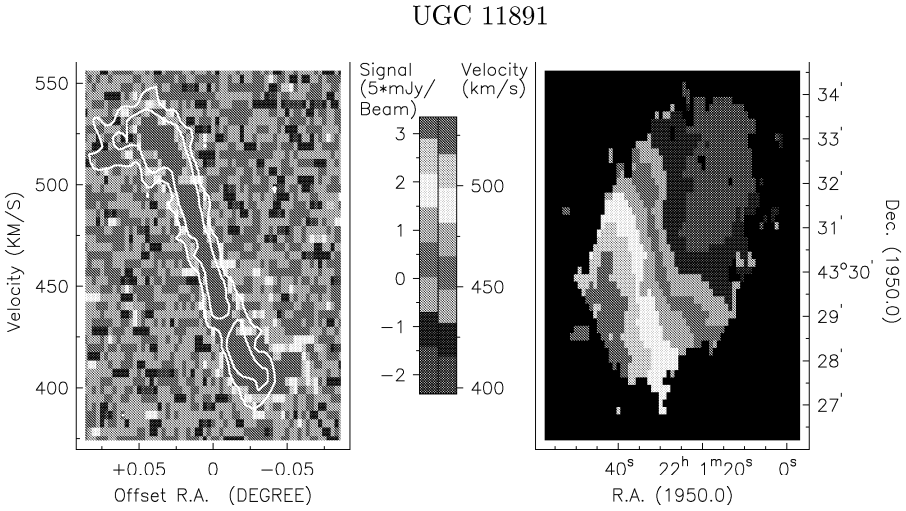

Figure 7: UGC 11891

The 1 σ level for the position velocity diagram of UGC 11891 is 0.726 Westerbork Units. The contours plotted in the position velocity diagram show the 2 σ and 5 σ level. The inclination of the system is 44 degrees.

Note: The dots in the position-velocity diagram represent the adopted rotation curve, hence not the independent rotation curve per side.

The overall quality of the position velocity diagram is poor and hence no conclusions can be drawn about the inner regions of the diagram. The turnover on both sides is quite comparable though the turnover on the right side is a tad bit closer to the center then that of the left side, compare the red area to the contours. Only the outer regions of the diagram show a distinct sign of a lopsided system. The right sight flattens off before decreasing while the left side decreases immediately after the turnover. UGC 11891's velocity field, however, shows the distinct signs of lopsidedness. The contour curvature on the receding side is almost absent while the approaching side contour curvature is high. A warp signature, the "s"-shape of the minor axes, border of both green parts, and the "s-"-shape of the major axis of the system is present. This helps to show once more that lopsidedness and warps are two completely different effects that can be found in the same disk galaxies.

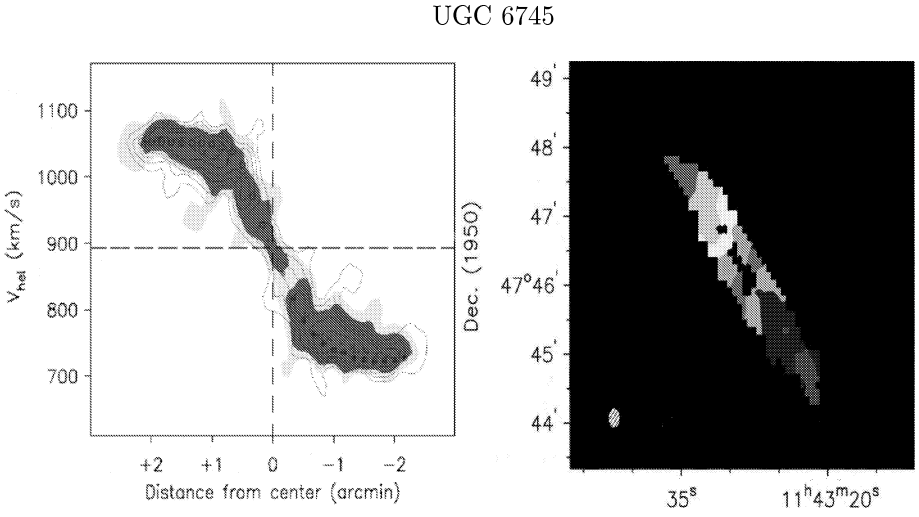

Figure 8: UGC 6745

UGC 6745's position velocity field data from 1.5 to 3σ is yellow above 3σ is red. The velocity field contains data from 700 km s^{-1} to 1100 km s^{-1} from purple till red in bins of 50 km s^{-1} width centered at 893 km s^{-1}, excluding the purple and red end bins, which contain data below 843 km s^{-1} for the purple bin and above 1043 km s^{-1} for the red bin. The inclination of the system is 81 degrees.

UGC 6745's position velocity diagram has been adopted from Verheijen's PhD. Thesis (1997) its inner regions are highly asymmetrical. The receding velocity side flares out heavily especially in the 1.5 to 3σ region of the diagram compared to the approaching velocity side. However when one looks at the velocity field one sees there is data missing in the inner regions of the diagram. Since the original data is not available for reinterpretation the possible effects this could or could not have had on the position velocity diagram inner regions remains unknown.
The turnover of the receding velocity side seems the smoothest of the two velocity sides but both velocity sides show an abrupt change in the velocity increase per arcmin. The approaching side either has two turnovers or a turnover followed by a smooth transition to the outer velocity. Appearance shifting from the first to the latter for low to high σ levels.
The receding velocity side has a slightly increasing slope while the approaching velocity side flattens off to a constant velocity.

UGC 6745's velocity field has been adopted from Verheijen(PhD. Thesis, 1997). It has been adapted to match the colour scheme used for the systems that were acquired from WHISP. The curvature on the receding

velocity half of the velocity field shows a flat trend except for the transition from the yellow to orange bin. There seems to be an expansion of orange into the yellow area, an underlying smooth curve seems to be present. The approaching velocity half of the velocity field has a large curvature for the transition regions between bins.

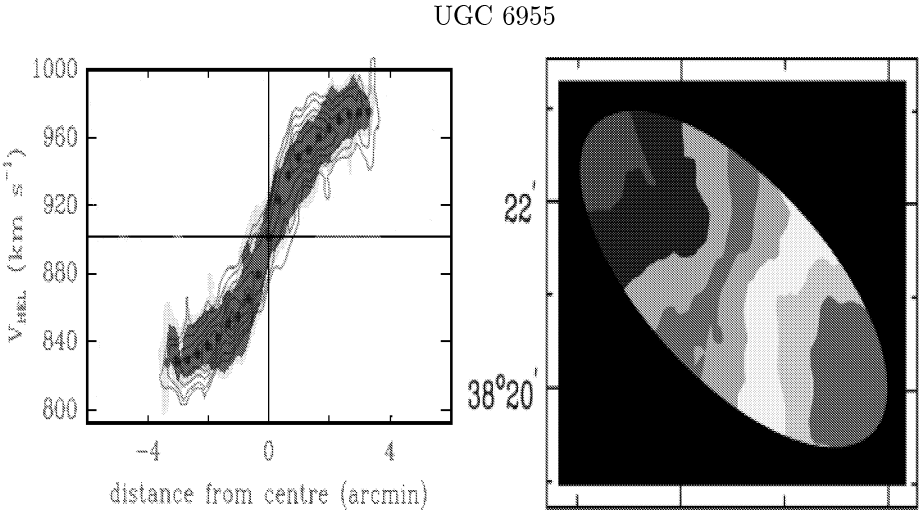

Figure 9: UGC 6955

UGC 6955's position velocity diagram data from 2.4 to 4.9K is yellow, above 4.9K is red. The velocity field contains data from 810 km s^{-1} to 1000 km s^{-1} from purple till red in bins of 20 km s^{-1} width centered at 900 km s^{-1}, excluding the purple and red end bins, which contain data below 840 km s^{-1} for the purple bin and above 960 km s^{-1} for the red bin. The inclination of the system is 73 degrees.

UGC 6955's position velocity diagram has been adapted from Broeils(PhD. Thesis, 1992) its inner regions extend somewhat farther out on one side then the other. The angle under which it extends is however similar for both the approaching as receding side. The turnover in the position velocity diagram is a smooth transition from the inner rotation velocities to the outer rotation velocities on the receding velocity side and a reasonable abrupt transition for the approaching velocity side. The outer regions show a flattening off of the velocities for the receding velocity side and a constant increase for the approaching velocity side.

UGC 6955's velocity field has been adapted from Broeils(PhD. Thesis, 1992) and adapted to fit the colour scheme used for the systems acquired from WHISP. To make this colour scheme possible an ellipse was fitted to the contours. Small extrapolations were necessary for some isovelocity lines in the original diagram as well as an extension of the data in the outer bins. These extrapolations however do not influence the general curvature of the isovelocity lines and velocity bins as can be seen in the figure.
The curvature of the velocity bins on the approaching velocity side is larger then the curvature of the receding velocity side bins.

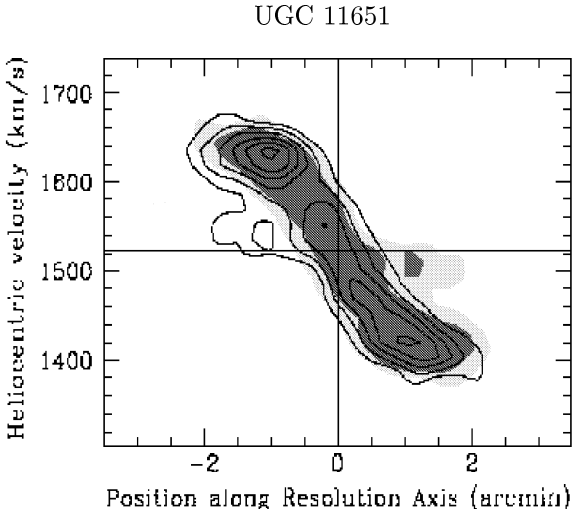

Figure 10: UGC 11651

UGC 11651's position velocity field data from 2.0 to 4.0σ is yellow, above 4.0σ is red. The inclination of the system is 90 degrees.

UGC 11651's position velocity diagram has been adapted from Rhee(PhD. Thesis, 1996) its inner regions are rather symmetric but for an extension of HI gas on the approaching velocity side of the system. The extension however doesn't seem to influence the general shape of the diagram. The approaching velocity side of the system suffers from a more abrupt turnover from inner to outer velocities then the receding velocity side. The outer regions show a larger flattening off for the receding velocity side then the approaching velocity side. However none of the velocity sides flattens of completely.

2.3.2 General properties of the strongly lopsided systems

Selection of systems by eye is highly likely to be biased towards certain differences which appear more strong to the eye then others while they in reality do not differ in strength at all. As mentioned previously the selection of the systems in this thesis suffers from the same drawbacks. With this in mind the ten strongly lopsided systems presented in section 2.3.1 were presented in such a way that the differences between the two velocity sides of a galaxy are enhanced to the reader. This is done without or even while suppressing the overall focus on these differences.

With the presentation of the ten studied systems chosen as described, the common properties that emerge should be considered a general trend indicative of lopsidedness, this not only in strongly lopsided systems but of course also in weakly lopsided systems.

But do we see common properties in the position velocity diagram and velocity field? Does our determination of what are lopsided systems and what not by looking at the position velocity diagram hold up? Are the two sides always different?
The answer to this question is: "Yes". The approaching velocity side of the position velocity diagram is always different from the receding velocity side of the position velocity diagram. But what are these differences and how common are they?

There are two differences between the approaching and receding velocity sides in the position velocity diagram that are clearly visible in all ten systems presented in section 2.3.1.

The most obvious of these two is a difference in the slope of the outer reaches of the position velocity diagram. This difference in slope however does not seem to be bound to a specific set of possibilities, like a flattening of on one velocity side and a continuing rise on the other velocity side. For example for the ten presented systems in section 2.3.1, there are two systems with two decreasing velocity sides and two systems with two increasing velocity sides.

The second difference is also quite easy detectable but quite difficult to quantitatively analyze since it can be highly influenced by manipulating the stretch of the x-axis compared to that of the y-axis. This second difference is the turnover from the inner velocity parts of the diagram to the outer velocity parts of the diagram. The curvature of this turnover differs from one velocity side to the other. If not for UGC 3137 one could have suspected at first glance from the ten systems studied that at least one velocity side has an abrupt turnover while the other side has a smooth transition from inner to outer velocities. Due to the representations chosen it is possible to establish that UGC 6745 and UGC 10359 however have one abrupt turnover on one side and

two, somewhat smaller in angle, abrupt turnovers on the other side. So UGC 3137 is not the odd one out and signifies one way to deviate from this picture established at first glance. The difference between the two turnovers ranges for our ten studied systems from two different abrupt ones to two different smooth ones. The difference between the two velocity side turnovers is something however all the ten systems studied share and hence a identifier in the position velocity diagram that a system is lopsided.

The inner regions of the velocity diagrams do not always show signs of lopsidedness. Due to the used method of aligning the center of the transposed image, contour levels, with that of the colour scheme level image one can not guarantee that there is not a slight offset created between the contours and the colour scheme. Hence an offset between the extension of gas on one side of the center in the colour scheme compared to the contour levels should be treated with consideration. This however does not affect the slope of the angle of the center of the contours and the colour scheme. Any form of misalignment will be a translation in the x,y-plane without rotation and hence the two slopes should be parallel. So one can state that most of the ten systems studied appear lopsided in their center parts of the position velocity diagram but that some are clearly not lopsided and hence the inner regions of position velocity diagrams should not be used to identify lopsidedness.

Next to the position velocity diagrams the velocity field belonging to nine of the studied ten systems was examined. Velocity fields should in the ideal symmetric case for a system be symmetric when rotated over 180 degrees. Therefor only the position of gas moving at a certain speed can be used as a tracer of lopsidedness when looking at the velocity fields. Velocity fields are limited in their use by their inclination, there is an upper limit to this inclination as well as a lower limit. The upper limit is around 80 degrees, the lower limit around 30 degrees, this due to errors introduced by random motions present in the gas in the system on the line-of-sight velocity. Also random motions combined with the width for the velocity channels of the original observation limit the accuracy of the velocity field, especially in the inner regions.
The inclination limits make the velocity fields of three systems not meaningful to study. The remaining six fields show however all the clear traces of asymmetry. The curvature of the isovelocity lines clearly differs between the approaching and receding velocity halves of the velocity field.
The isovelocity lines curvature is for these systems in cases so extreme one velocity side has highly parabolic curvature compared to the almost flat curvature of the other velocity side, UGC 7524 and UGC 10359 are nice examples of this.

Next to the inclination being a limiting factor on the identification of lopsidedness in systems the location of the assymetries in the system are of importance. If the assymmetries are located near or on the the minor axis

instead of the major axis the lopsided effects will be much harder to detect and might even be missed. The curvature of the iso-velocity lines at the center of a "normal" velocity field is much less then that of the iso-velocity lines for the maximum and minimum velocities. Causing assymetries to have a much lesser impact on the velocity field in the inner then outer regions.
The importance of this effect is shown by Swaters(1999) in figure 3 of chapter 5. Here he shows the position angle of a studied system is important for how lopsidedness shows in a velocity field. These effects can not be taken into account when studying the system by eye and hence the much more moderate asymmetry in the zero position angle example is much more easily missed then the asymmetry in the 90 degree position angle example.

From the study of the position velocity diagrams one can conclude that lopsidedness is quite easily detectable in position velocity diagrams. The tell trace sign being an asymmetric approaching and velocity side in the position velocity diagram. This asymmetry consist of a distinct difference between the outer slopes of the position velocity diagram and a difference in the transition from the inner to outer parts of the diagram. The difference in the transition most likely being a difference between a smooth and abrupt turnover.

The velocity field by itself is limited in use by an upper and lower limit on the inclination and a possible cover up of the traces for lopsidedness. However it is an excellent tool to support the findings of lopsidedness in a position velocity diagram, especially in the cases of a favorable position angle and inclination angle. In which case there is no mistake possible in identifying the difference between the approaching and receding velocity sides asymmetry.

Studying the (physical) parameters presented in table 3 and comparing them to the same parameters but than of a number of symmetric systems does not show significant differences between the symmetric and lopsided systems. This comparison however is done with a small amount of systems and hence the creation of a larger control sample built up out of symmetric systems to compare with the lopsided sample is desireable.

2.4 Control sample

As mentioned in section 2.2 to be able to compare strong lopsided systems to not strong lopsided systems a control sample was created. The systems that were put into the control sample were selected from the WHISP database. From the total list of galaxies a random number of galaxies were selected which did not match any of the criteria, see section 2.2 on page 8, on which Sancisi's sample was based. This was done to ensure no misidentification in the type of lopsidedness could corrupt the sample. Also this enhanced the chances of finding differences between the strong lopsided sample and control sample. The criterion for selection was the morphology of the systems involved. The original sample contains systems ranging in morphology from Sbc to Im, this

also includes the barred and intermediate cases. Classification of systems by eye is more an art then a science according to many but classifications by different experienced astronomers often leads to about one class in type difference. The author reclassified all systems in the WHISP database and found that only in 5% of the cases he differed more then one whole class type from the WHISP classification. Therefore the control sample is extended to contain the Sb group next to all the groups present in the original sample. An extension to the other side of the Hubble diagram is not necessary since the original sample already contains irregulars. The distribution of the morphological types of the lopsided sample compared to the distribution of the morphological types of the WHISP database is shown in figure 11.

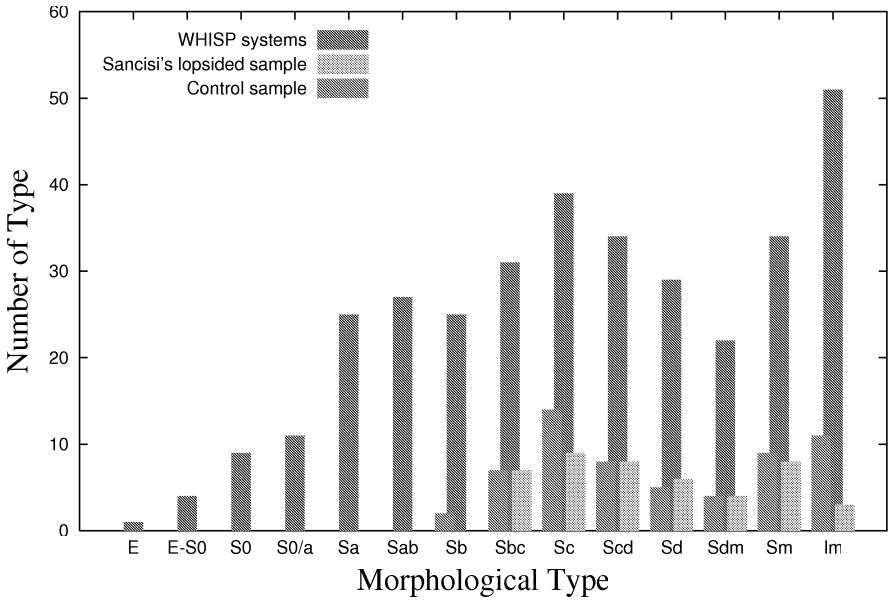

Figure 11: Distribution over the morphological types for the lopsided Sancisi sample, control sample and the WHISP database

Of all 388 systems present in the WHISP database(mind that the present day distribution can look somewhat different due to a number of systems added) subdivided over 19 different classes only the total number of 342 systems have been plotted in the histogram, for the remainder of the systems no morphological classifications were available. Also some morphological classes were combined for convenience, for example the lenticular group normally consists of three types whereas here we just show all lenticulars grouped together.

Figure 11 shows that Sancisi's lopsided sample matches the distribution over

the different classes present in the WHISP database for the types of systems present in the sample except for the irregular group. This deviation in the amount of systems present in the lopsided sample compared to that of the WHISP sample in the Irregular group is most likely explained by the irregularities present in Irregulars, which makes identification of lopsidedness extremely difficult or simply impossible and hence the under matching of the amount of detected lopsided Irregular systems.

From the similar distribution over the morphological classes for the systems present in the lopsided Sancisi sample and the WHISP database we infer that our sample is not morphologically biased and that a comparison of the lopsided sample with a control sample built up out of a selection of systems from the WHISP database is viable.

The system selection for the control sample will be done randomly and is expected to match that of the WHISP database within errors. The randomness of selection secures that no dependence on parameters is introduced, except of course the limitations posed by the WHISP sample itself. The similarity in morphological distribution over the classes present in both the lopsided Sancisi sample and the WHISP database allows for the same similarities between the lopsided Sancisi sample and the control sample. The classification used in the control sample is based on classifications found in Tully's Nearby Galaxies Catalogue (1988) and in LEDA, to be able to compare it to the lopsided Sancisi sample for which the classifications are based on these two sources and the four PhD. Theses used.

Figure 11 shows that the control sample morphological distribution matches that of the WHISP sample and hence that of the lopsided Sancisi sample.

The data for the systems in the control sample can be found in table 9.

3 Discussion

In this section the main (physical) parameters for systems present in the lopsided sample and controlsample from chapter 2 will be examined. In seven graphs a set of these parameters will be represented in a "morphological type-parameter" comparison per sample.

3.1 Tables

3.1.1 Parameters

Both the control sample, see table 9, and the lopsided Sancisi sample, see table 10, contain 15 columns of parameters collected from the sources mentioned in the section 2. The parameters are chosen to give a basic overview for a galaxy. Some parameters are complementary in nature some overlapping, e.g. M_{HI} or M_{tot} are complementary and epsilon and d25(') or epsilon and the inclination are overlapping. The reason for including overlapping columns of parameters is based on the unambiguous approach of astronomy towards standards. Some astronomers prefer one representation, e.g. epsilon, some others, e.g. the inclination. In table 5 each parameter column is explained. For a detailed list of the used sources for the lopsided Sancisi sample see table 4 on page 12.

System	:	All systems are present in the UGC database (Nilson, 1973) opposed to other databases and hence are all identified with their UGC number.
Type	:	Based on the coding of revised morphological types.
D25(')	:	Also referred to as the optical diameter in many databases this is the major axis length of a system in the blue visual spectrum or B-band.
d25(')	:	The minor axis length of a system, like the D25('), in the blue visual spectrum or B-band.
ϵ	:	The ellipticity of the system. The ellipticity is mathematically calculated by: 1 - d25(')/D25(') and hence ranges theoretically from 0 to 1 for edge-on systems to face-on systems. However in practice this is never achieved due to several astronomical effects, e.g. dispersion velocity, and the ellipticity ranges not much higher then 0.8. This effect is plotted in figure 39 on page 83 and as shown depends on the morphological type of the system.
Inclination	:	The inclination is calculated via the ϵ, the correlation can be found in figure 39 on page 83.
m_B	:	Apparent corrected magnitude in the blue part of the visual spectrum or B-band.
M_B	:	Absolute corrected magnitude in the blue part of the visual spectrum or B-band.
L_B	:	Luminosity in the blue part of the visual spectrum or B-band in units of the solar luminosity in the B-band.

Distance	:	Distance in mega parsecs. For the control sample this is corrected for the infall of the local group towards the Virgo cluster for the lopsided Sancisi sample this depends on the angle as described in the NGC (Tully, 1988).
M_{HI}	:	Logarithm of the total corrected neutral hydrogen gas mass represented in solar unit masses. In both the control sample as in the lopsided Sancisi sample LEDA is used after attempts to convert each independent source that has data on the neutral hydrogen masses proved too time consuming.
M_{tot}	:	Logarithm of the total mass of a system.
ρ	:	Density of galaxies per megaparsec cubed. Based in both the control sample and lopsided Sancisi sample on the NGC (Tully, 1988).
Group	:	Taken from the NGC (Tully, 1988).
Companion	:	Based on a multitude of sources, like NED(NASA/IPAC Extragalactic Database) and the SIMBAD database. The area that is queried in SIMBAD is based on the distance of the system and a maximum line-of-sight velocity of 300 km s^{-1}.

Table 5: Parameter list for table 9 and table 10

Due to the parameters for the lopsided Sancisi sample being selected mainly from the PhD. Theses mentioned in section 2.1 this data is the most up to date available. It however lacks an uniformity we would like when comparing it to other samples. This problem is partly resolved by adapting the numbers to one standard but most often this lack of uniformity has to be accepted.

For the control sample the LEDA database is used. The number of systems present in other sources then LEDA were too low to forsake uniformity and error data for the sake of higher quality data.

3.1.2 Sample comparison

The history of comparing (physical) parameters samples in astronomic research has shown that most (physical) parameters suffer from weak correlations for the group of the late type galaxies. This correlation continued to remain weak even when sample sizes increased over the years. However per morphological type there seems to be an upper and lower limit for each parameter. Where this limits, and the conclusions that can be based upon them, are dependent on the biases present in the studied samples.
One of the largest sample comparisons is presented in an article by Roberts & Haynes (1994). In this paper they present over 15 physical parameters for the

samples studied. Since a part of their sample is based on the UGC database (1973) we will use their result as a reference for the plots which will be generated in this thesis.

In this thesis we will look at the correlation of 7 (physical) parameters with the morphological type. This 7 parameters are the L_B, M_{HI}, M_{tot}, M_{HI}/L_B, M_{tot}/L_B, D25 and ρ. In comparative plots in the paper by Robert & Haynes (1994) it is shown that per morphological type the samples are statistically skewed. Since our samples are considerably less populated then those of Robert & Haynes (1994) we should expect our samples to be skewed also and thus that for the (physical) parameters we will have to consider the effects that has on the statistical representation we chose for the data. This means that both the average and the median will have to be calculated and compared with and as in Robert & Haynes (1994). If we see comparable differences we can use their results to support our results. In each of the 7 figures the skewness is represented by the different values for the average and median plotted for a morphological type. Also as in Robert & Haynes (1994), per morphological type, the errorbars represent for the upper errorbar the 75-th percentile range and for the lower errorbar the 25-th percentile range. The reader should be aware that for a few bins there are only two or three systems that occupy that particular bin and hence this has consequences on the percentile ranges.

The average in the 7 presented graphs will be represented by an open square while the median will be represented by a filled circle. The percentile ranges will be centered on the median values since we expect our samples to be skewed. Each parameter will be shown as an average over all systems, presented per morphological type.

In figure 12 the relation for the linear diameter(kpc) is shown. We expect a slowly declining trend for the diameter when moving to later types. This trend is visible in both this thesis and Robert & Haynes (1994), though in Robert & Haynes (1994) one needs to compare to log of the linear radius.

In figure 3.1.2 the relation for the local density(Gal./Mpc^3)is shown. This parameter is not present in Robert & Haynes (1994). The density tells us something about the chances for encounters between systems that could cause lopsidedness in those systems. We do not expect to find a specific trend. More massive systems tend to be less easily disturbed and hence show lopsided effects, also they tend to survive longer then smaller systems which will be more likely to be accreted. Numerically however the late type systems have the advantage. For all three samples the density does not fall outside of the range of another sample. There is no trend visible between the control sample and the lopsided sample, both groups seem to occupy roughly the same density regions of space.

In figure 3.1.2 the relation for the logarithm of the blue-band luminosity(solar

luminosities) is shown. A decreasing trend is expected towards the later type systems due to the presence of dwarf systems, see also Robert & Haynes (1994). This trend is found in our graph, no sample falls outside the range of one of the other samples. The only noteworthy deviation in this graph is the much lower average and median value for the "Sm" type systems in the lopsided sample. This is due to one systems with a very low luminosity which influences the skewness of the sample significantly.

In figure 3.1.2 the relation for the logarithm of the neutral hydrogen gas mass(solar masses) is shown. Later type systems contain in general less mass then the earlier type systems within the spiral group. Both our graphs as those of Robert & Haynes (1994) show this trend clearly. Again the only deviation between the three samples is found in the "Sm"type morphological group within the lopsided sample and again it is the sample system that causes this group to lie considerably lower due to its much lower then average mass.

In figure 3.1.2 the relation for the logarithm of the total mass(solar masses) is shown. As with the neutral hydrogen mass graph we expect a decreasing trend in the total mass toward the late type section of the graph. We again see this in our graphs and that of Robert & Haynes (1994). As with the last two graphs the deviations between the samples fall within the respective ranges of the other samples. Again the "Sm" type morpholical group shows the largest deviations, this time however both the lopsided sample and strong lopsided sample contain one system that deviates strongly from the average.

In figure 3.1.2 the relation for the logarithm of the neutral hydrogen gas mass devided by blue-band luminosity is shown. There is a slightly increasing trend in both Robert & Haynes (1994) graphs and ours. Since this relationship is a quite complicated no prove that it should be expected in our graph can be given. The deviations are what we expect(including the deviations for the "Sm" morhological type systems in both the lopsided and strongly lopsided sample) when we look at the previous graphs.

In figure 3.1.2 the relation for the logarithm of the total mass devided by the blue-band luminosity is shown. When comparing the graph of the total mass with that of the blue-band luminosity it becomes apparent that both have a quite similar shape. Therefor a flat distribution is expected for the total mass over luminosity graph. Since both of these graphs are similar in Robert & Haynes (1994) paper we expect to find the same flat distribution also in their total mass over luminosity graph, which we do. As in the neutral hydrogen gas mass over blue-band luminosity graph both the "Sm" type morphological lopsided groups show the largest deviation from standard, though as expected.

Comparing the represented parameters presented in each of the 7 graphs per sample over all morphological types shows no significant differences between the three samples. The differences that are found, per morphological type,

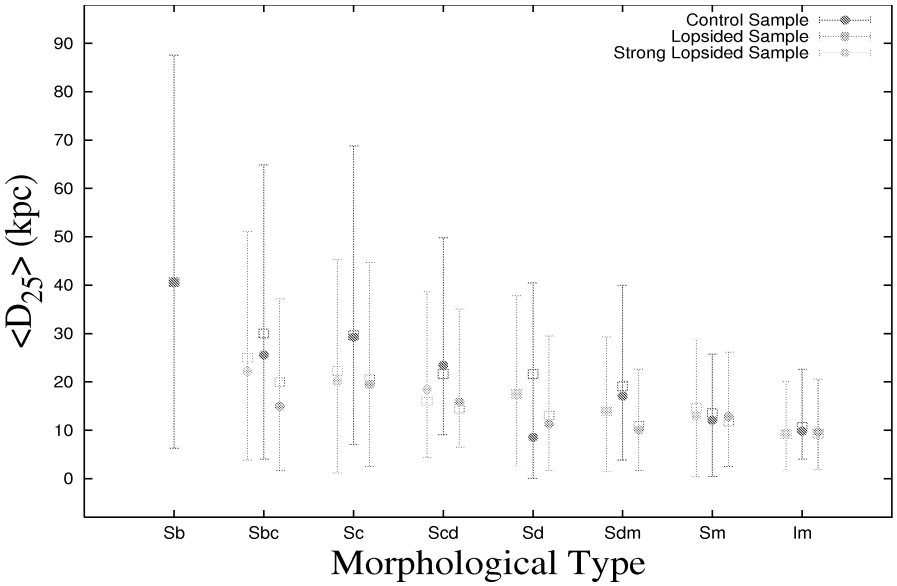

Figure 12: Optical linear diameter in arcminutes vs. morphological type for the Control Sample, Lopsided Sample and Strong Lopsided Sample. Average values are represented by open squares, the median values are represented by filled circles. The errorbars represent for the upper bar the 75th percentile en for the lower bar the 25th percentile.

between a parameter in one sample compared to that same parameter in one of the other samples(e.g.: lopsided sample versus control sample) are not repeated. Neither are these differences repeated in the neighbouring morphological type of the same sample. When comparing the data in the 7 graphs with similar data in the paper of Robert & Haynes (1994) we see that for the different morphological types there are no significant differences between the graphs. All of the 3 samples presented in this chapter behave as expected within the limits defined by the percentile ranges. From this comparison we can conclude that our sample is skewed but does not suffer from underpopulation. Hence does not make the skewness significant enough to be unable to draw conclusions from our graphs.

The conclusion that we therefor draw from the examination of the 7 presented graphs is that the (physical) parameters for the lopsided, strongly lopsided and control sample do not significantly differ between those samples. We however note that our sample does suffer from undersampling, but comparison with the results presented in Robert & Haynes (1994) shows no large differences between the results for the presented samples in this thesis and their work.

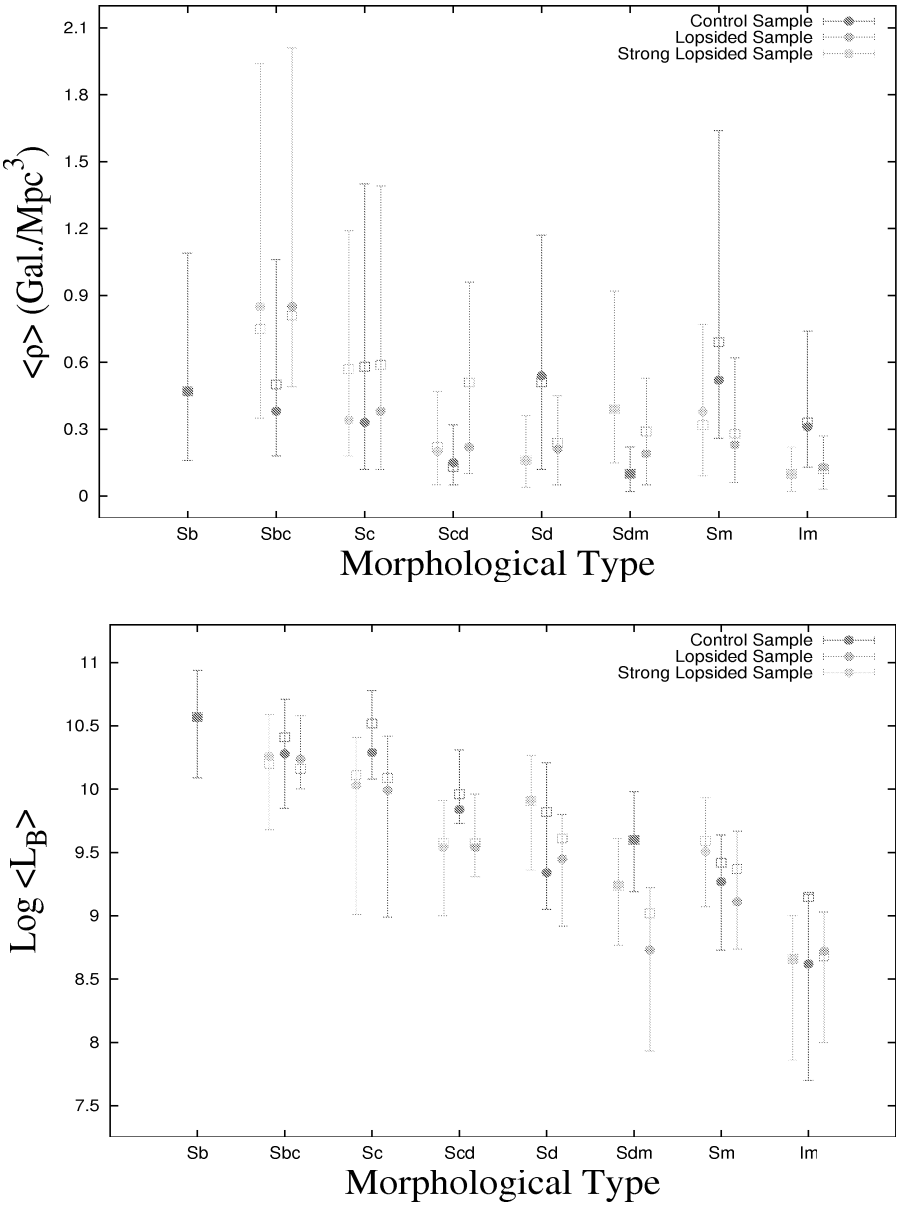

Figure 13: Top : Local density in galaxies per cubed megaparsec vs. morphological type, Bottom : Logarithm of the B-band luminosity expressed in solar units vs. morphological type, for the Control Sample, Lopsided Sample and Strong Lopsided Sample. Average values are represented by open squares, the median values are represented by filled circles. The errorbars represent for the upper bar the 75th percentile en for the lower bar the 25th percentile.

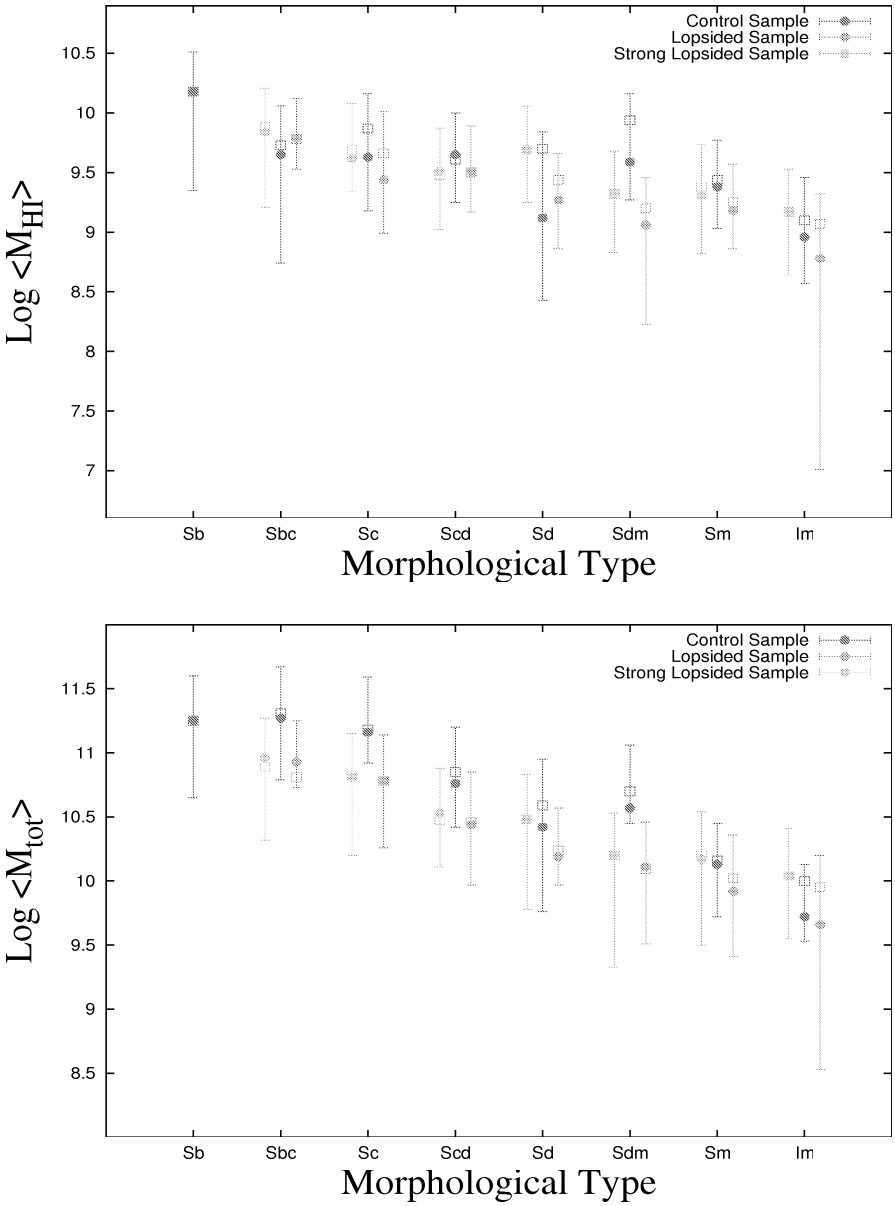

Figure 14: Top : Logarithm of the neutral hydrogen gas mass expressed in solar units vs. morphological type, Bottom : Logarithm of the total mass, based on W20, expressed in solar units vs. morphological type, for the Control Sample, Lopsided Sample and Strong Lopsided Sample. Average values are represented by open squares, the median values are represented by filled circles. The errorbars represent for the upper bar the 75th percentile en for the lower bar the 25th percentile.

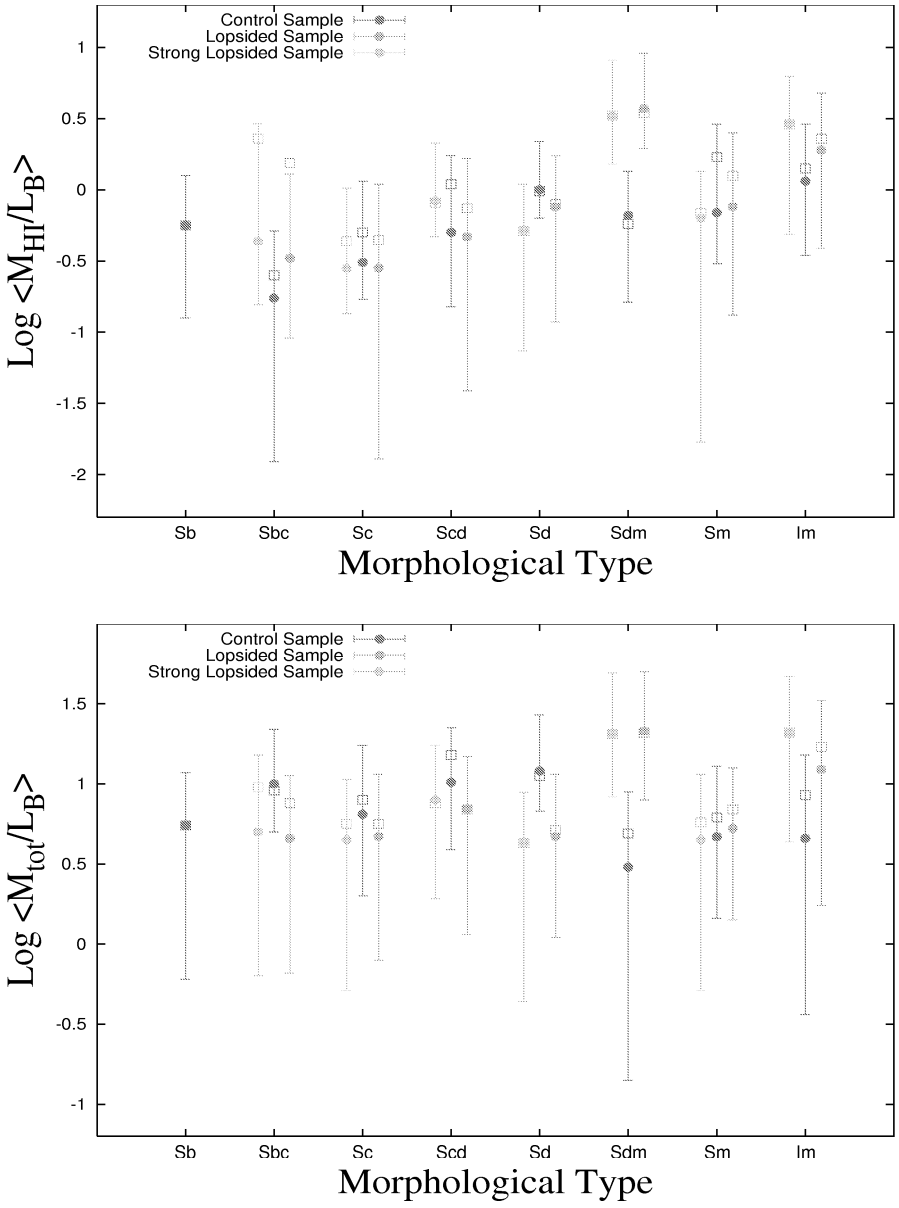

Figure 15: Top : Logarithm of the neutral hydrogen gas mass over the B-band luminosity expressed in solar units vs. morphological type, Bottom : Logarithm of the total mass, based on W20, over the B-band luminosity expressed in solar units vs. morphological type, for the Control Sample, Lopsided Sample and Strong Lopsided Sample. Average values are represented by open squares, the median values are represented by filled circles. The errorbars represent for the upper bar the 75th percentile en for the lower bar the 25th percentile.

4 Improving on the control and lopsided sample

In this chapter we will use the key elements that point towards lopsidedness determined in section 2.3.1 to improve, with the help of the WHISP database on the sample s presented in chapter 3. As in chapter 3 we will present and compare our results in a set pf 7 "morphological type"-parameter graphs.

4.1 Obtaining the improvements

In chapter 3 the original lopsided sample provided by Prof. Dr. R. Sancisi was compared to a control sample that was built up by a random selection of systems based upon the WHISP database. The control sample in this comparison however was subject to possible contamination by weakly lopsided systems. Also both the control and lopsided sample were undersampled.
In this chapter a new lopsided sample and control sample are created based upon the WHISP database which do not suffer or suffer less from the aforementioned problems of the samples used in chapter 3.
To improve on the conclusions that can be drawn from the study of the control sample and the lopsided Sancisi sample in chapter 3 a tool to identify lopsidedness is needed which does not suffer from the drawbacks such as that suffered by the global profile, which up till now is most often used to identify lopsidedness. For the global profile both the density distribution and the kinematics of the neutral hydrogen gas can compensate for each others perturbing presence in global profiles hence lopsided systems can be overlooked. Also there is no clear definition of when the kinematic and density distribution for a specific system point towards a symmetric system or a weak lopsided system. The lack of this definition is what makes control samples likely to be corrupted with weakly lopsided systems next to the symmetric systems they are built up out of.
This possible confusion of symmetric control samples makes comparison of physical parameters between symmetric systems and lopsided systems as a whole difficult since the significance of this confusion can not be determined due to the lack of statistics on the occurrence of lopsidedness per morphological type.

However our study of ten strongly lopsided systems, see section 2.3.1, offers us a system which seems to be solid enough to overcome the problems posed to us by the global profile.
If we use the position velocity diagram together with the difference in the slopes of the parts of diagram as described in section 2.3.2 to determine the lopsidedness of a system we avoid the chance that the density distribution and the kinematics of the neutral hydrogen gas compensate for each others influence in the representing diagram next to using a method which seems to be able to point out strong lopsidedness and most likely lopsidedness in

general.

Next to a method to determine lopsidedness in a system a bigger sample is needed to reach a higher level of confidence in our previous results. This coincides with the need to test our hypothesis that the method to identify lopsidedness that we determined from our study of the ten strongly lopsided systems is solid enough to be used as an identification method for lopsidedness.

The WHISP database contains far more systems than both the control sample and the lopsided Sancisi sample together and therefor will be used for this purpose. However the WHISP database contains only 388 systems of which a significant number will be unusable for our purposes while we would prefer a database of about 660 systems with 30 systems per morphological type varying from "Sa/0" to "Im". The author tried to find other databases but found not a single database that would serve this purpose without requiring a considerable amount of work to fit the purposes of this thesis. However it is safe to assume a significant improvement will occur in the number of the systems present in samples built up out of all systems present in the WHISP database compared to the old control sample and lopsided Sancisi sample.

Culling of the systems present in the WHISP database to prepare the database for identification purposes lead to the direct removal of 46 systems, those systems were either double present or had, sadly, data of extremely poor quality, read non existent. Another 111 systems were deemed not suited for identification purposes. A myriad of reasons were the cause of this de-selection, e.g.: Too poor resolution, too high noise levels, heavy disturbances present due to interactions.
The removal left 233 systems which the author deemed suitable for identification with the developed method.

For all the 233 systems a quick assessment by eye was done based on the difference in the slopes between the low and high velocity halves of the system in the position velocity diagram. The slopes for both the inner and outer part of the position velocity diagram were compared as well as the turnovers on both velocity sides. If the system was clearly lopsided the neutral hydrogen gas fields and velocity fields were immediately assessed. It was determined if there was lopsidedness detectable by eye in either the neutral hydrogen gas field or the velocity field or both and if so it was cataloged.
The remaining systems were studied in more detail, first the position velocity diagram was blown up in size and parallel lines were drawn, with the help of a plotting tool, to allow for a better comparison of the slopes of the low and high velocity halves in the position velocity diagram. If a system, after this simple test, was found to be lopsided its neutral hydrogen gas fields and velocity fields were studied and any detected lopsidedness was cataloged. If the system was found to be not lopsided by this simple method a final determination was done based on transposed contours overlapping the position

velocity diagram. Akin to the method used in section 2.3.1. Detected lopsidedness was treated as described previously and lopsidedness in the neutral hydrogen gas fields and velocity fields was cataloged.
All the systems remaining after these three tests are considered to be not lopsided or symmetric in their position velocity diagram. These systems however are not considered symmetric before they are tested for signs of lopsidedness in their neutral hydrogen gas fields and velocity fields. If lopsidedness is detected in one of the fields this is cataloged and the system is removed. All remaining systems hereafter are considered to be symmetric and will make up the new control sample.

The new control sample contains 81 systems, a 35 percent increase over the old control sample, spread over morphological types "S0$^-$ to "Im". The new lopsided sample contains 131 systems, a 191 percent increase over the old lopsided sample, spread over morphological types "S0$^-$, "S0$^+$", "Sa" to Im. Next to these two samples there remain 21 systems that are either lopsided in their neutral hydrogen gas fields or velocity fields or both but possess a symmetric position velocity diagram. These 21 systems will be excluded from the review of the new lopsided and new control sample.
This systems do show that there is a limit to the used method developed to identify lopsidedness. Even if for a number there is an explanation why their position velocity diagrams most likely do not show signs of lopsidedness there remain several systems that show no signs of lopsidedness in their position velocity diagrams while they do in either velocity fields or neutral hydrogen gas fields.

The distribution over the morphological types per sample is shown in figure 16. In contrast to figure 11, see page 29, there should not be a similar match per morphological type between the three represented samples in figure 16. The cause for this being that the systems are not random selected from a master sample but the whole master sample is split up over different morphological type bins. Figure 16 should show us the percentile distribution over the morphological type for the control sample and lopsided sample. Previous work by for example Matthews et al.(Matthews et al., 1998b) hint that lopsidedness should occur more frequently towards the end of the Hubble fork. This means that for the later type systems in figure 16 the percentage of lopsided systems should increase compared to the percentage of systems in the control sample. The numeric distribution over the morphologic types of the lopsided and control sample compared to the total number of systems present in the WHISP master sample, represented in percentages, is shown in table 6. Table 6 shows there is an increase in the percentage of lopsided systems towards later types but it is neither a smooth increase nor does it hold for the irregular group and "Sab" group. For the morphological type groups "Sa" to "Scd", excluding the "Sab" group, the lopsided systems make up on average 58 percent of the sample while for the morphological type groups "Sd" to "Sm" the lopsided systems make up on average 76 percent of the sample.

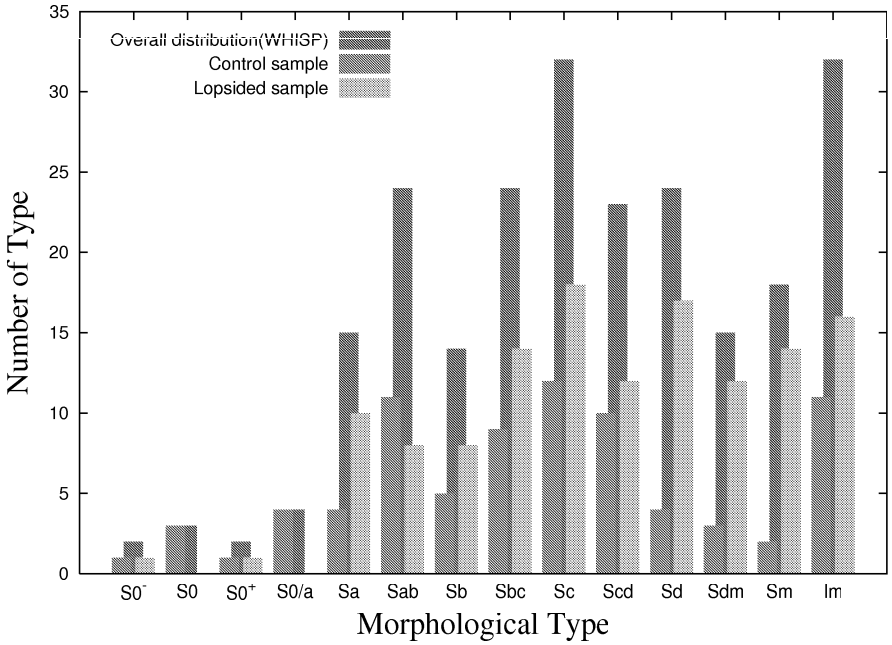

Figure 16: Distribution over the morphological types, "Sa" to "Im" for systems present in the WHISP sample(233 usable systems for identification), the new control sample and the new lopsided sample

Overall it seems that at least 50 percent of the field galaxies is lopsided as was also found by Richter & Sancisi (1994) and Haynes et al. (1998) and that late type systems seem more likely to be lopsided then earlier type systems with the break in the distinction in how high a percentage of the systems is lopsided being between the "Scd" group of galaxies and the "Sd" group of galaxies. The irregular group of galaxies seems to be a case by itself.

To test the identification method used to identify lopsidedness by the author a comparison was made of the results acquired by using this method and the identification results of the lopsided Sancisi sample, see table 1, on page 9. The determination if systems were lopsided in the WHISP master sample(233 galaxies) was done, by the author, independently from their UGC identification number. This insures both samples have their lopsided classifications determined independently.
Of the 45 systems present in table 1, 5 systems were classified differently. Of these 5 systems one system, UGC 6869, was not classified(uncertain classification) in the lopsided Sancisi sample, one system, UGC 6251, was not present in the WHISP master sample due to poor data quality, one system, UGC 1249, is noted to be disturbed by a companion galaxy and two are actually classified wrongly. The two wrongly qualified systems are UGC 7075,

	Sa	Sab	Sb	Sbc	Sc
Lopsided sample	66.67	33.33	57.14	58.33	56.25
Control sample	26.67	45.83	35.71	37.50	37.50
Rest	6.67	20.83	7.14	4.17	6.25
	Scd	Sd	Sdm	Sm	Im
Lopsided sample	52.17	70.83	80.00	77.78	50.00
Control sample	43.48	16.67	20.00	11.11	34.38
Rest	4.35	12.50	0.00	11.11	15.63

Table 6: Percentage of systems in the lopsided sample and control sample compared to the WHISP master sample.

which was classified symmetric by using the method developed by the author while being classified weakly lopsided in the lopsided Sancisi sample. The other system is UGC 1501, which is classified as being lopsided by using the method developed by the author while it is being classified not lopsided in the lopsided Sancisi sample.
After careful review the author reached the conclusion that both systems were identified with the help of overplotting transposed contours and that in both cases it was this method that forced the decision if the system was classified lopsided or not. Since the classifications in the lopsided Sancisi sample were reached by study of the position velocity diagrams and velocity fields by eye compared to the classifications reached by using the method the most likely reason is simple misclassification in the lopsided Sancisi sample.
However if even these two misclassification's are included the method seems to identify lopsidedness with at least an 95 percent accuracy in the position velocity diagrams.

The accuracy we got for classifying when building up the sample was 91%. So for the WHISP database the lower limit when classifying the systems in this database is around 90%. When classifying other samples, the obervational limits of the WHISP database will have to be compared to that of the studied sample. Physical similarities between the samples will have to be proven for this lower limit to hold true for the sample under study.

Having created, within the limits of the data used, a symmetric control sample with a low chance of confusion by weakly lopsided systems, a comparison of 7 standard parameters for the systems present in both the control and lopsided sample will be made as well as a comparison for the mass-to-luminosity relationships, as in chapter 3. The results for the parameter-morphological type comparison are presented in figure 17, figure 18, figure 19 and figure 20.

4.2 The results

The overall increased size per morphological type bin over both samples, mind that for example the "Sm" bin for the control sample went from 9 to 2 systems, leads clearly to a better structural agreement with the results from Robert & Haynes (1994). The peak in the $<D_{lin}>$, $<L_B>$, $<M_{HI}>$, $<M_{tot}>$, $<M_{HI}/L_B>$ and $<M_{tot}/L_B>$ values for all graphs lie for this thesis and Robert & Haynes (1994) work around the morphological "Sb" type. This could not be confirmed from the graphs presented in chapter 3. The numeric values representing the parameters also match much tighter then they did in chapter 3.
Skewness for the new sample is clearly of lesser influence although it still is significant enough to influence the spread plotted in the parameter type comparison graphs.
The conclusion that was drawn in chapter 3 based on the parameter type comparison graphs presented there becomes only more evident. Lopsided spiral galaxies do not differ significantly from their symmetric counterparts when comparing basic physical parameters, neither do they occupy a higher density region of space compared to their symmetric brethren.

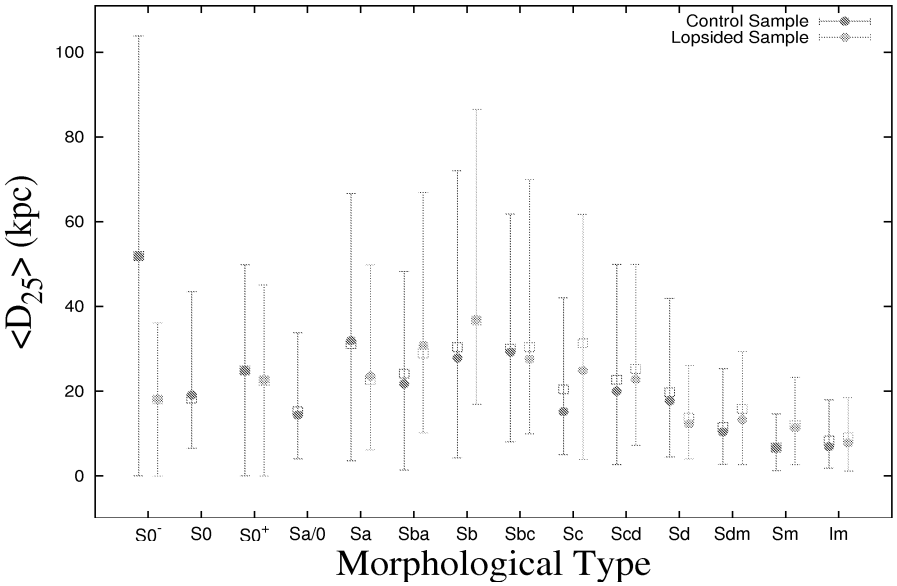

Figure 17: Optical linear diameter in arcminutes vs. morphological type for the Control Sample and Lopsided Sample. Average values are represented by open squares, the median values are represented by filled circles. The errorbars represent for the upper bar the 75th percentile en for the lower bar the 25th percentile.

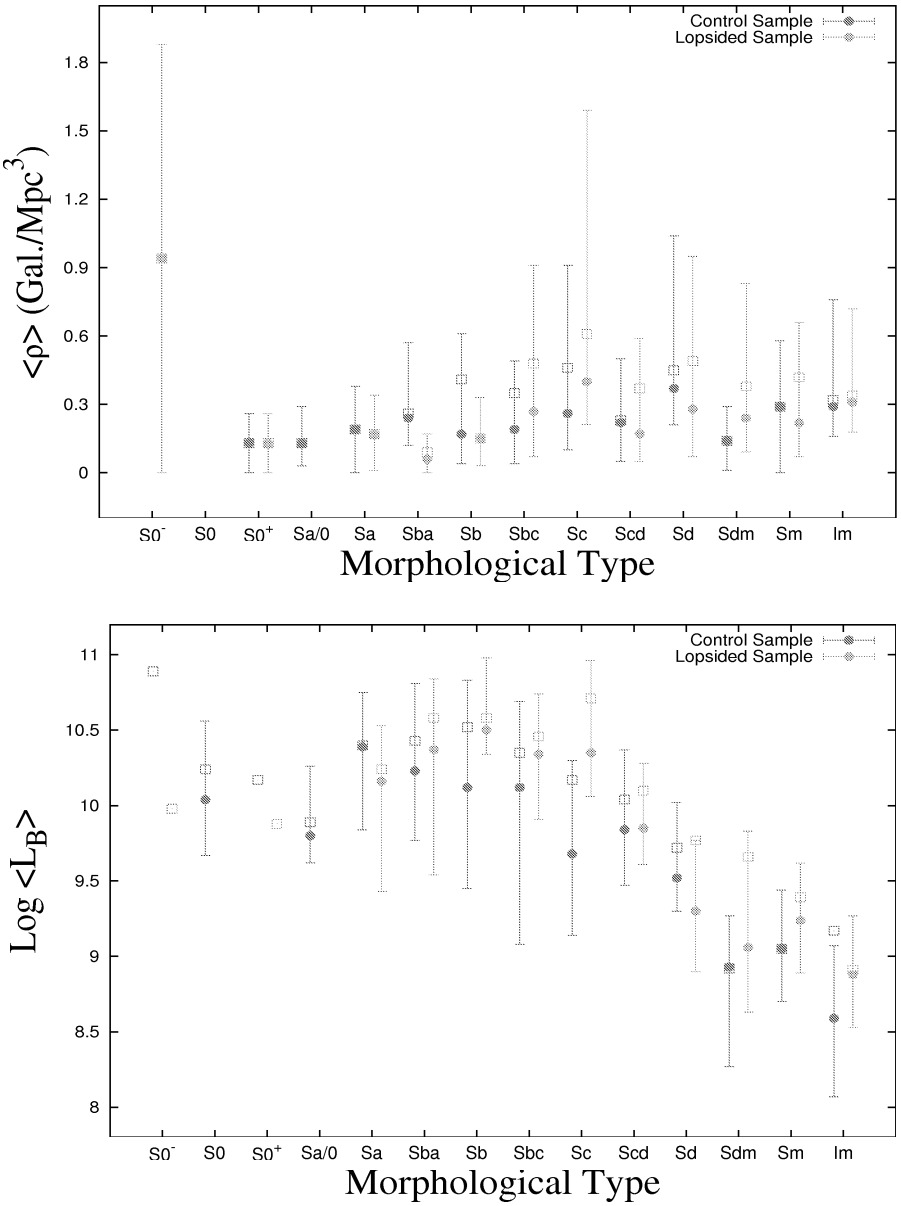

Figure 18: Top : Local density in galaxies per cubed megaparsec vs. morphological type, Bottom : Logarithm of the B-band luminosity expressed in solar units vs. morphological type, for the Control Sample and Lopsided Sample. Average values are represented by open squares, the median values are represented by filled circles. The errorbars represent for the upper bar the 75th percentile en for the lower bar the 25th percentile.

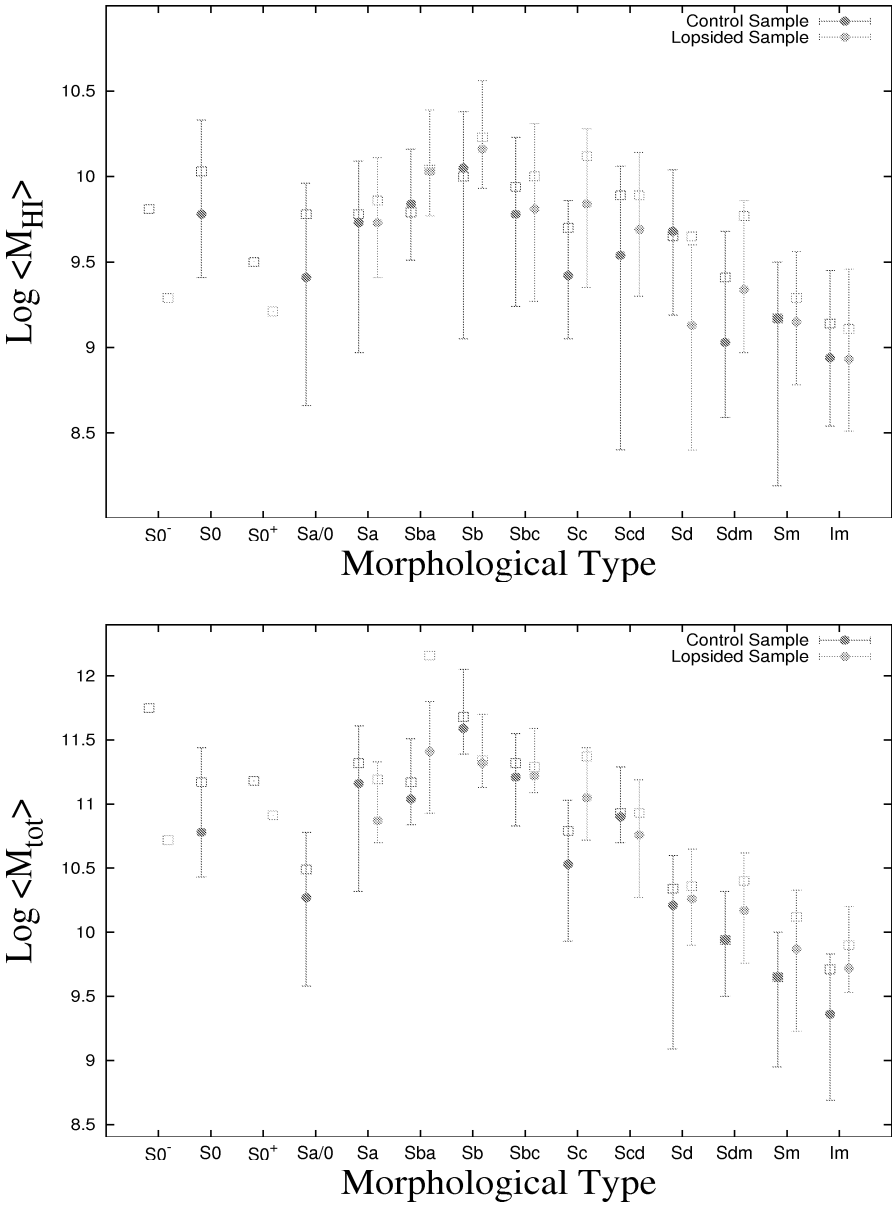

Figure 19: Top : Logarithm of the neutral hydrogen gas mass expressed in solar units vs. morphological type, Bottom : Logarithm of the total mass, based on W20, expressed in solar units vs. morphological type, for the Control Sample and Lopsided Sample. Average values are represented by open squares, the median values are represented by filled circles. The errorbars represent for the upper bar the 75th percentile en for the lower bar the 25th percentile.

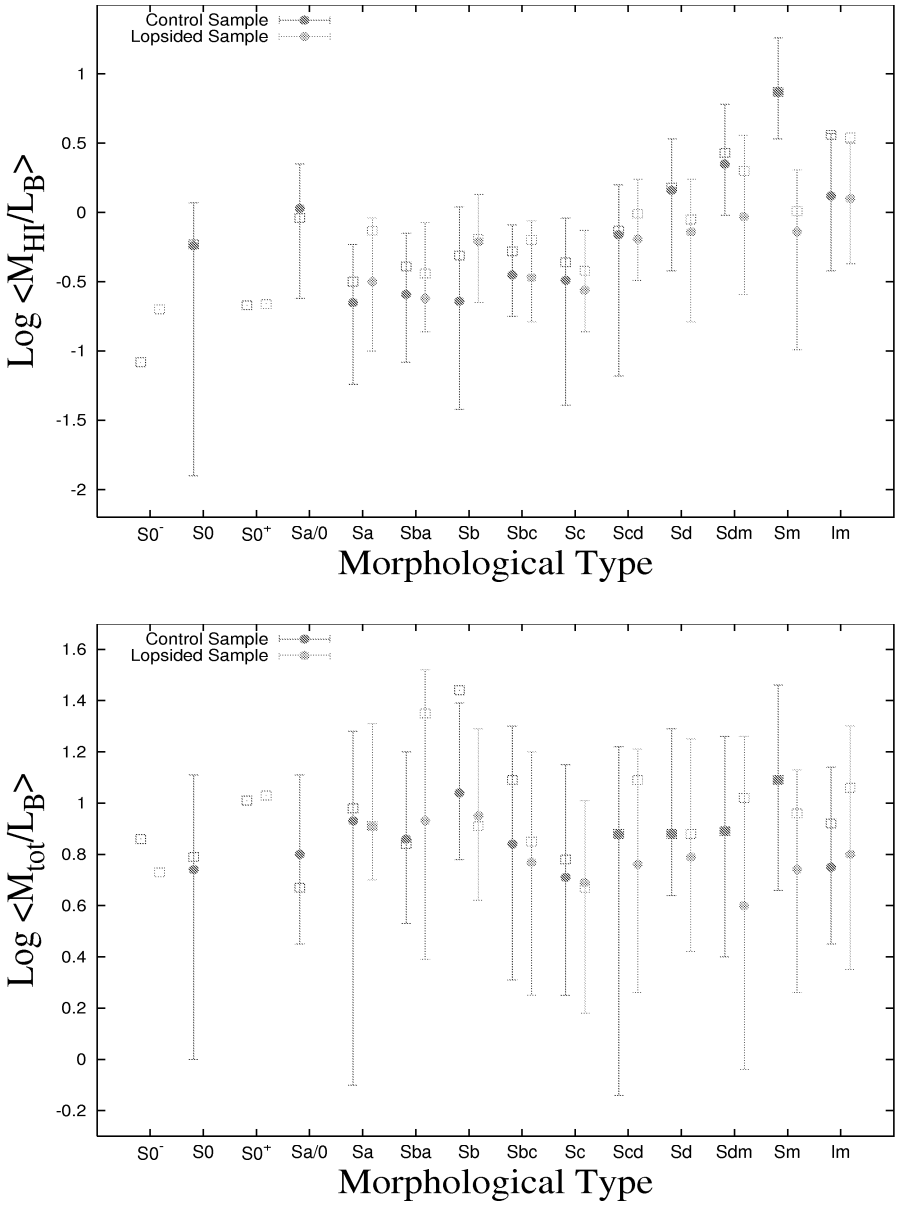

Figure 20: Top : Logarithm of the neutral hydrogen gas mass over the B-band luminosity expressed in solar units vs. morphological type, Bottom : Logarithm of the total mass, based on W20, over the B-band luminosity expressed in solar units vs. morphological type, for the Control Sample and Lopsided Sample. Average values are represented by open squares, the median values are represented by filled circles. The errorbars represent for the upper bar the 75th percentile en for the lower bar the 25th percentile.

5 Conclusions

When Richter & Sancisi(1994) found that over 50 percent of the about 1700 galaxies in their studied sample had a asymmetric global profile, lopsidedness became an undeniable effect that affected spiral galaxies as a group and not the odd individual.

Already explanations for lopsidedness had been presented before their publication and more would be after it, studies in more and more detail with increasingly accurate models describing the cause and strength. However a study into the properties of lopsided galaxies as a group was still lacking.

This Master Thesis presents data on 45 lopsided galaxies and 60 symmetric galaxies collected from a number of databases and PhD. Theses in chapter 3. From this data no differentiation between the two samples could be found. Hence lopsided galaxies show no differentiation from symmetric galaxies in their general properties.

Global profiles are a good tool to identify lopsidedness, but lopsidedness however can be missed using global profiles. As a study into a better method to identify "kinematical" lopsidedness the attention was drawn to the position velocity diagrams of strongly lopsided systems. From a study of ten strong lopsided systems the conclusion is drawn that position velocity diagrams are an excellent tool to identify "kinematical" lopsidedness. Even under a very simple representation of the position velocity diagram and under circumstances that suppress the focus of ones eyes on the characteristics of lopsidedness in the position velocity diagrams all ten systems show the tell trace signs of lopsidedness. All systems clearly show a different angle for the slope of the outer regions of the position velocity diagram when one compares the approaching and receding velocity halves. Also the transition regions from the inner part to the outer part of the velocity diagrams differ clearly between the approaching and receding velocity halves.

For nine of the ten strongly lopsided systems studied, velocity fields were present or could be retrieved. Due to limiting factors as an upper and lower limit on the inclination and a bias on how lopsidedness shows in velocity profiles the use of velocity fields is limited to a supporting role of the position velocity diagrams. The six remaining velocity fields however clearly show the effects on lopsidedness when one studies a velocity field. One side of the velocity field clearly has a much more flat curvature for the isovelocity lines then the other velocity side.

The weakly lopsided systems present in the original sample provided by Prof. Dr. R. Sancisi also show the same telltale traces of lopsidedness as the 10 strongly lopsided systems that were reviewed in detail. Therefor the use of the position velocity diagram to identify lopsidedness, may it be weak or strong,

seems to be a quick and extremely easy method.

Using the position velocity diagram method, to identify lopsidedness, all the systems present in the WHISP database were reclassified anew, leading to a new lopsided sample containing 131 systems and a new control sample containing 81 systems. Comparing the identification of the systems present in the original lopsided sample provided by Prof. Dr. R. Sancisi to their new identification lead to the conclusion that the position-velocity diagram method level of accuracy lie just below the 2 σ level. Using the developed method also means that the unknown confusion of the old control sample with weakly lopsided systems is kept to a minimum.

The conclusions that can be drawn from the results based on the new lopsided sample and new control sample are however not different from those which can be drawn based on the older samples. It can even be said with greater confidence that the represented parameters show no significant difference between symmetric and asymmetric or lopsided systems.

One of the main causes for lopsidedness in systems is assumed to be interaction with other systems or more often accretion of small companion systems. The local density, ρ, which represents the environmental conditions for the systems did not show significant differences between the lopsided systems and the symmetric systems. An attempt was made to see if a direct search for companions could be used to eliminate one of the possible outcomes for this question. This however turned out to be impossible. Searching for companions turned out to be a too time consuming affair, as samples are most often observational limited and we are also dealing with very late type systems, the chances that small companions that would be able to disturb these low mass systems are missed is just simply to big.
However of the earlier type systems, “Sa” to “Scd”, when using a lower mass limit of 10%, of the mass of the system under review, for a companion, a significant amount has no nearby companions.

To further the knowledge of lopsided systems and the cause of lopsidedness, systems are needed that are lopsided throughout a range of frequency bands. One of these systems is UGC 731, a classical example especially for the position velocity diagram, another is UGC 7090, which is a stunning example of how lopsidedness can affect a system. In the data panels presented on the WHISP homepage one can clearly see the lopsidedness in each panel. The optical figure has a huge gap in the southwestern section, like a pizza-slice taken out, the global profile fits all three the criteria for lopsidedness stated in Richter & Sancisi (1994), the position velocity diagram shows asymmetry in the inner and outer region as well as the transition region, the HI panes show missing HI on the spot where the optical figure also lacks it stars and the velocity field is a good example how the curvature of the isovelocity lines differ when comparing velocity halves.

However the presentation does not match the quality the data for UGC 7524 has. The high spatial resolution that is reached for UGC 7524 is also needed to study lopsidedness in UGC 7090 in particular and in other systems in general better then is allowed now.
General properties of lopsided systems do not seem to differ between these asymmetric galaxies and their symmetric counterparts though we clearly see differences in both the kinematical as well as the HI column density within those galaxies. Hence a more in-depth review is necessary to unravel this apparent contradictions, to confirm or deny this uniform appearance in general properties between the lopsided and not lopsided galaxies and point the way for future research and model creation to explain the causes of lopsidedness.

In the parameter-type graphs no division was made per morphological type between barred and not barred systems. Dividing each morphological type group into a barred and not barred group would have simply spread the number of systems available to us, in the samples, out to thinly to determine any meaningfull statistics. However it is possible to look at the division of the barred and not barred systems as two individual groups. If we split up the WHISP database we find that 58% of all systems is barred. Repeating this for the symmetric group of systems in the control sample, from chapter 4, we find that 48% is barred while for the lopsided group from the lopsided sample we find that 70% is barred.
The reason for this difference being so large is unknown to the author of this thesis neither are there any previous written papers the author found that mention a difference between the percentage of barred systems in a lopsided sample compared to the percentage of barred systems in a symmetric sample. If the difference in the percentages of barred systems between lopsided and symmetric systems holds for several samples this however might prove why lopsided systems seem to be a bit brighter in the blue band when compared to symmetric systems. The same seems to hold true for barred systems, which also appear to be a bit brighter in the blue band then their none barred counterparts. In figure 18 we see that on on average the value for the medians of the lopsided sample are higher then the values for the medians of the controlsample, however we are not able to confirm this trend since these average values fall within the error ranges we use.

A Galactic Introductory

This chapter contains a low level introduction to the subject of galaxies and lopsidedness, combined with a small historical introduction. For the experienced reader it may function as a small reminder of what the basis behind the research of the subject of this paper is.

A.1 Galaxies

```
Webster's Revised Unabridged Dictionary (1913):

Galaxy \Gal"ax*y\, n.; pl. Galaxies. [F. galaxie, L. galaxias,
   fr. Gr. ? (sc. ? circle), fr. ?, ?, milk; akin to L. lac. Cf.
   Lacteal.]
   1. (Astron.) The Milky Way; that luminous tract, or belt,
      which is seen at night stretching across the heavens, and
      which is composed of innumerable stars, so distant and
      blended as to be distinguishable only with the telescope.
      The term has recently been used for remote clusters of
      stars. --Nichol.
```

The use of the word recent is more appropriate then one would think at first sight. Galaxies are such an important part of today's Universe that one almost would forget that it is no more then fifty years ago astronomers really started to understand that galaxies are the building blocks of the Universe and that a century ago our Universe only existed out of the stars inhabiting the Milky Way, our own galaxy.

To be historical correct one needs to mention that the idea of different galaxies was already mentioned by Kant in the eighteenth century. In 1610 Galileo discovered that the Milky Way was not a "river of milk" as the Greeks and Romans thought but a band of faint stars. Kant used this knowledge combined with the appearance of our own solar system, the planets rotate in a disk around the Sun, to come up with the idea that our own galaxy should be a huge rotating disk like object build up out of stars. He suggested that other objects on the sky which were clearly not stellar, referred to as nebulae, could be distant stellar systems like our own. It was William Parsons who for the first time made a drawing of a spiral galaxy around the half of the nineteenth century. With the introduction of photographic plates a much better reliable method for measuring luminosities was introduced at the end of the nineteenth century. With the possibility to measure luminosity of objects much better a

somewhat strange path led to the determination that some of those nebulae must be objects very far away from our own Milky and hence must be other systems that resembled the Milky Way.

The astronomer Kapteyn used photographic plates in huge quantities to make a stellar count of the sky. By measuring the proper motion, small shift in position of a star on the sky over the years, and determining how stars were related from one to the other(the brightness of a star diminishes if that star is placed further away or it could be a less brighter star), Kapteyn could make up a picture of the stellar system we lived in. This picture is referred to as the Kapteyn Universe. Around the same time the astronomer Shapley studied globular clusters, this are spherical systems with 10^4 up to 10^6 stars. The none uniformity in the distribution of these globular clusters led Shapley to devise a model that consisted of a sphere full of globular cluster with in the center the Milky Way itself.

Kapteyn's universe was so different from Shapley's universe that it led to a discussion amongst astronomers which one was the right view. Shapley's Universe was ten times larger then Kapteyn's Universe and it was reasoned was large enough to be the whole universe. The Kapteyn Universe couldn't contain those nebulae, if it was assumed the nebulae were intrinsically the same size their difference in size would be explained by a larger distance. Since certain nebulae were over hundredth times larger then others they would have to lie outside the Milky Way. This made the Kapteyn Universe quite a bit larger then Shapley's Universe though for which no explanation was given. The debate lasted until Edwin Hubble, five years later, determined that the distance to one of the most luminous nebulae, M31(the Andromeda galaxy), was some 300 kpc(62 billion times the distance to the sun). Since the Andromeda Nebula was one of the biggest and brightest on the sky a lot other much smaller nebulae would have to be many times farther away. Hence the start of the present view of how our universe is build up was formed. A large expanse filled with both spiral nebulae or spiral galaxies and elliptic nebulae or elliptical galaxies.

The years after the conclusion of the debate, Edwin Hubble continued to study other galaxies and catalog them. Thirteen years later Hubble published "The Realm of the Nebulæ" (1936), in this work he introduces a classification scheme for galaxies, see figure 21. Hubble suggested galaxies evolved from the left-hand side to the right. Elliptical galaxies would slowly transform to spiral galaxies. Therefor Hubble referred to elliptical galaxies as early type galaxies and spiral galaxies as late type galaxies. Hubble's idea of galaxy evolution has by now been refuted and replaced by an evolution idea based on merging of smaller systems into larger.
After Hubble passed away different astronomers continued to work on his legacy, which culminated in "The Hubble Atlas of Galaxies" (1961) and an adaption of his classification scheme, in which his hypothetical lenticular group

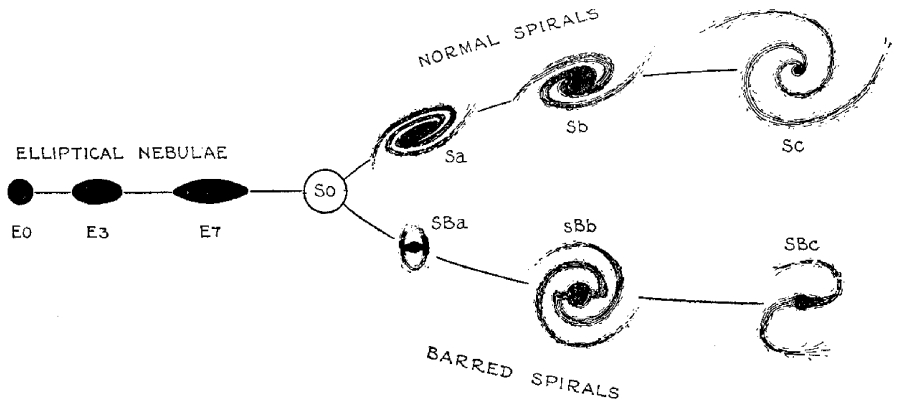

FIG. 1. *The Sequence of Nebular Types.*

The diagram is a schematic representation of the sequences of classification. A few nebulæ of mixed types are found between the two sequences of spirals. The transition stage, S0, is more or less hypothetical. The transition between E7 and SB_a is smooth and continuous. Between E7 and S_a, no nebulæ are definitely recognized.

Figure 21: The Hubble tuning-fork diagram from The Realm of the Nebulæby Edwin Hubble, 1936

of galaxies became a real group with a subdivision of three types.
The most elaborate adaptation was made by de Vaucouleurs (1959) in which he adds two extra spiral classes and in which he completely adapts Hubble's Irregular classification. de Vaucouleurs classification scheme is at the moment the most complete scheme available to astronomers. However even de Vaucouleurs scheme is not fully complete. In recent years a group referred to as dSph, dwarf spheroids, has been peeking more persistently around the corner. These are extremely small spiral or elliptical galaxies which are difficult to detect especially at large distances, even by modern technological standards, and hence their importance in the classification scheme is still unknown.

Even if Hubble's classification scheme has been adapted over the years and the final the Vaucouleurs classification scheme doesn't include each known system the basis laid down by Hubble is considered solid. There are four main groups in which galaxies are fitted: Elliptical-, Lenticular-, Spiral- and Irregular Galaxies. For each group of galaxies there is a set of features that each galaxy in that group satisfies. In the next section a number of these features will be discussed.

Hubble:	E	E-S0	S0	S0/a		Sa	Sa-b	Sb	Sb-c		Sc		Sc-Irr		IrrI	
Vaucouleurs:	E	$S0^-$	$S0^0$	$S0^+$	S0/a	Sa	Sab	Sb	Sbc	Sc	Scd	Sd	Sdm	Sm	Im	I0
T:	-5	-3	-2	-1	0	1	2	3	4	5	6	7	8	9	10	0

Table 7: Different morphological classification types and there corresponding number(T)

Astronomers can determine the type of any galaxy by the use of the above three parameters determine quite accurately. Though they often disagree not more then a whole type it is not strange to find classification who differ as far as Sb to Sm.

The T numbers in table 7 are the Hubble stage numbers of the galaxies based on de Vaucouleurs scheme.

A.2 Ellipticals

Figure 22: M 87, type cD

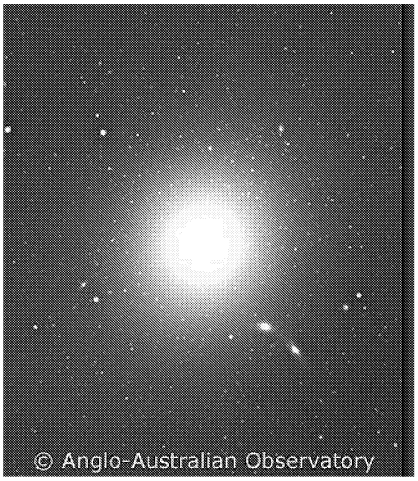

Figure 23: NGC 4742, type E4

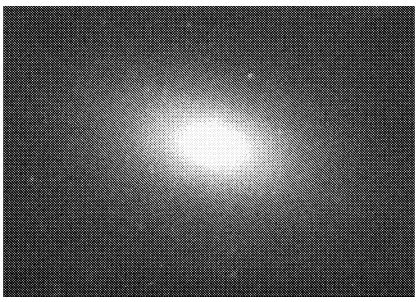

Figure 24: NGC 3193, type E2

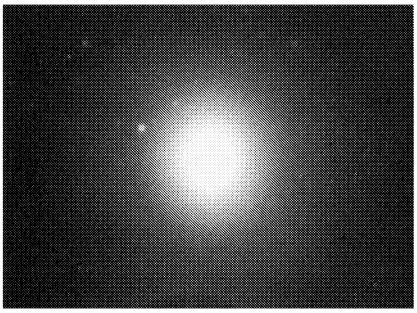

Figure 25: NGC 4564, type E6

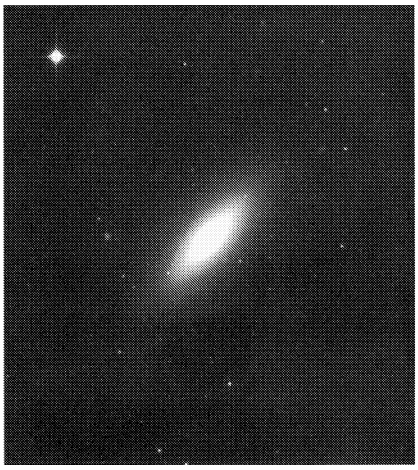

Figure 26: Pictures of these galaxies are copyrighted to the AAO

The group of elliptical galaxies is build up out 8 types of different elliptical shapes, dwarf ellipticals and a "cD" identification for giant ellipticals, giant ellipticals reside in the interior of very galaxy rich "clusters of galaxies" and are the product of numerous mergers of galaxies. The other 8 types of ellipticals are numbered from 0 to 7 which is based on their increasing flatness.[6] Meaning an E0 galaxy comes closest to a perfect sphere while an E7 galaxy looks more like a big cigar. Elliptical galaxies tend to reside in the high density regions of the universe. Around 50% of galaxy clusters centers is made

[6]The E-number "x" is based on the ratio of their major and minor axis projected on the sky. The formula that goes with this is $x = 10(1 - b/a)$ where b is the minor axis and a the major axis.

up out of elliptical galaxies.
Ellipticals are mainly build up out of old, red, stars. Their light distribution is smooth and fades towards the outer edges of the system. The formula associated with this decline in surface brightness(luminosity per unit area) found by de Vaucouleurs[7] is $L(r) = L(0)e^{-(r/r_0)^{1/4}}$

Ellipticals are gas and dust poor and hence lack the ability to form new stars especially in the quantities spirals and irregulars can form them hence the smooth light distribution.

The shape of the elliptical is due to ratio of random motions compared to rotational motions. Ellipticals have little to no rotational velocities but large random velocities. The difference in shapes(E0 to E7) is due to an anisotropic velocity distribution. Stars move on average faster in one direction then the other, the larger the difference in velocity between the axial directions the flatter the distribution of stars and hence the shape of the system. See table 8 for some numerical properties of elliptical galaxies.

[7] r is the distance from the center of the elliptical along the major axis, r_0 is the scale length, the distance at which L(0) drops to $\frac{1}{e}$ or $\sim 37\%$; L(0) is the central luminosity of the galaxy.

A.3 Lenticulars

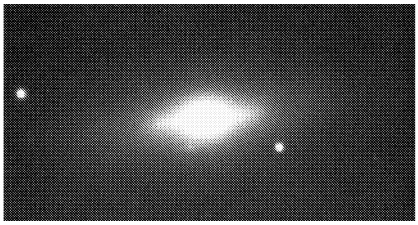

Figure 27: NGC 4251, type S0

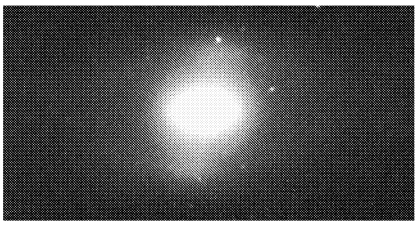

Figure 28: NGC 4371, type SB0

Figure 29: Pictures of these galaxies are copyrighted to the AAO

When moving from early type galaxies(ellipticals) to late type galaxies(spirals) one passes the group of lenticular galaxies. Lenticulars are a group of galaxies that combine elliptical features with that of spiral galaxies, it is believed that lenticulars are in some way remains of spiral galaxies that exhausted all their hydrogen gas by forming stars in the past or lost that gas by some other means so they could not form stars anymore. Lenticulars, like ellipticals tend to reside in the high density regions of the universe. However as the density of ellipticals decreases when moving to the outer edges of a galaxy cluster that of lenticulars increases till it peaks, followed by a rapid decrease.

Lenticulars are divided into two subgroups like spiral galaxies, normal and barred. Each of these two groups is subdivided into three different types based on different properties. The barred group devision is based on the prominence of the bar but that of the non-barred group is based on the prominence of the dust lane present.

The light distribution of lenticulars is dominated, like ellipticals, by a smooth central light distribution. But next to the elliptical light distribution the lenticulars have a slower declining distribution surrounding the central light distribution. This outer distribution has a disk likes structure however it shows no traces of spiral structure. This disks stars seem to rotate around the center of the lenticular galaxy in much the same way as star do in spiral galaxies. However in lenticular galaxies their orbits seem to be a bit more elliptic. Lenticulars seem to posses dust in different amounts but are almost always gas ridden. See table 8 for some numerical properties of lenticular galaxies.

A.4 Spirals

Figure 30: M 104, type Sa

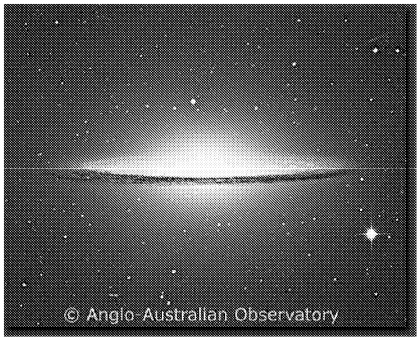

Figure 31: M 83, type SABc

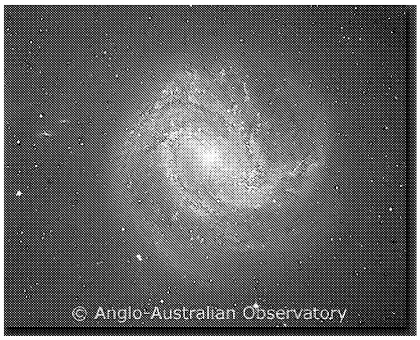

Figure 32: NGC 2841, type Sb

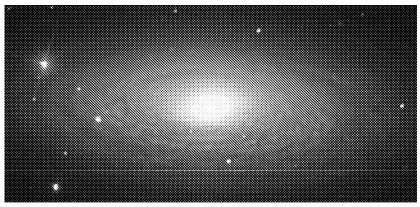

Figure 33: NGC 1365, type SBb

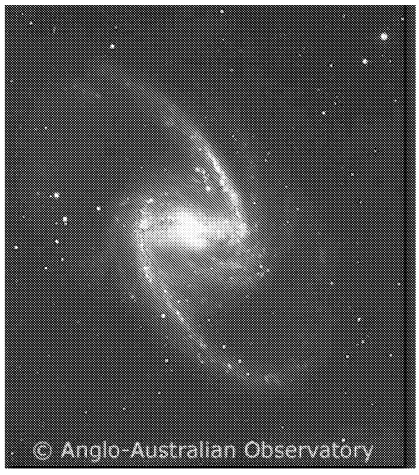

Figure 34: Pictures of these galaxies are copyrighted to the AAO

The most well known type of galaxy amongst the general public is not the most abundant but certainly the most diverse amongst it brethren. Spanning a whole range of different characteristics, from the large bulge and smooth arm like Sa-type to the almost irregular looking Sm-type, next to all those differences in bulge and disk shape they come with or without a bar at their center.

Spiral galaxies reside in the low density regions of the universe, in clusters they are mainly found in the outer edges of that clusters.

Independent of type and almost independent for the whole group of galaxies named spirals is their general build up. Spiral galaxies contain a bulge at their center and a flat disk surrounding the bulge containing one or more spiral arms. Though in some cases no bulge is found, this is however a very small

portion of all spiral galaxies and almost always in very late type systems.

The bulges in spiral galaxies resemble elliptical galaxies in more then one way, not only do they appear the same they also seem to obey to some of the same empirical laws. As with ellipticals de Vaucouleurs formula
$L(r) = L(0)e^{-(r/r_0)^{1/4}}$ is true for bulges. Bulges mainly contain, the old red, population II stars. However there are differences, for example rotational velocities in bulges are on average higher then that of ellipticals. The rotation in bulges almost always explains the flattening of those bulges.
The most striking difference is the possibility of a bar. Bulges may contain a bar like structure. This bar can extend beyond the bulge or be contained within the reaches of the bulge.

The disk in spiral galaxies is a very flat structure when compared to the bulge height and especially when compared to its radius. The disk of spirals differs from that of lenticulars in that it has structure, this structure is referred to as spiral arms. These spiral arms have a hugely varying appearance which differs from early type spiral galaxies to late type spiral galaxies. The arms can be almost smooth like or almost seem like beads on a string of small(Arp) where the beads are star forming complexes, they range from very broad to very tight and from red to blue in appearance.
Like with elliptical galaxies and bulges there is also a de Vaucouleurs law for galactic disks, $L(r) = L(0)e^{-r/r_0}$, for this formula it is presumed the stars are uniformly distributed over the disc, for which the stars in the spiral arms are smoothed out circularly over the disc.

The Hubble diagram explained above was as mentioned improved by de Vaucouleurs (1959) and it divides spiral galaxies according to their prominence of their bulges and the appearance of their spiral arms. More tightly woven smooth spiral arms belong to the early(Sa) type, combined with a large bulge, and more loosely wound clumpy arms belong to the later(Sd) type, combined with a small bulge or in some cases no bulge at all. Next to the overall light distribution of the bulge and disk importance and tightness of the spiral arms windings the resolution of the galaxy in separate stars or star forming regions(HII nebulae) is used to determine the type of a spiral galaxy.
Next to this the spiral galaxies are either barred, non-barred or an intermediate between barred or non-barred.

Why spiral galaxies possess a bar or not is still under debate. Both are about as equally common in the same type of universal environment. Causes are often searched in the direction of the huge dark halo's surrounding the galaxies which could support different kind of potentials needed to explain the difference.

The bar is the only real obvious visual difference between normal and

non-normal spiral galaxies, next to the color of the galaxies, on the grand scale. Most spiral galaxies possess two spiral arms which contain, dependent on the type, more or less star forming regions. Those star forming regions are dominated by extremely luminous, up to a million times the solar luminosity, stars. Luminous stars peak in brightness in the blue part of the spectrum. Normal stars, like the sun, who are most abundant in spiral galaxies are yellow-reddish of color. Hence this star forming regions add blue light to a yellow-reddish background. In general the later the type of galaxy the more star forming regions and the larger the bluer component in the total light distribution.

But why does a spiral galaxy have a spiral shape? Spiral arms of a spiral galaxy cannot be observed to move. Timescales for a galactic rotation are around several hundredth million years. Different explanations have been put forward over the years but up till now none seems to be able to explain the diversity seen among spiral galaxies in a single theory. The first theories make use of density waves and can be split up in different approaches.

The most well know is the Lin-Shu hypothesis (Lin and Shu, 1964) and (1966). It states that a spiral structure consists of a quasi-steady density wave which is maintained in a steady state over a number of rotational periods. Lin-Shu's theory explains why most spirals seem to have two arms and why most spiral arms seem to be trailing the direction of rotation of a galaxy. Also Lin-Shu's theory seems to explain the shape of the distribution of the red light of spiral discs well. This red light comes mainly from old disc stars which are the pre-dominant mass contributor to the discs total mass. Hence the surface brightness of the light is directly related to the surface density. Their density wave should therefor show in this red light, which is does. Also the theory explains the narrow, high-density gaseous arms very well which we in effect see as the small band of star forming regions in spiral arms.

The second theory that makes use of density waves is the chaotic spiral arms theorem. This theorem focuses on explaining the more ragged, loosely spiral armed galaxies which are more common then the grand-design spirals. The ragged structure is created due to local instabilities in the gravitational field. Stars form in these regions and then due to differential rotation this patch is sheared into the resemblance of a spiral arm. Many of these patches together give the galaxy a spiral shape. These arms are short lived and vanish due to continued shearing. Star formation is self regulating in this theory. Cooling and infall of material creates regions of gravitational instability which leads to star formation in these regions. The subsequent supernovae lead to heating of the surrounding and a stop to star formation. The arm then slowly dies out. Sellwood & Carlberg (1984) show that a self-regulating instability may be able to produce the structure seen in Sc-type of galaxies.

The third theory uses the effect of companion galaxies. Toomre & Toomre

(1972) modeled the M51 system by using this assumption. Their model predicts quite accurately what we see on the sky in reality but only for the outer regions of the discs. A possible explanation is given in Toomre (1981). Models that use tidal interaction are able to give an explanation as well as the Lin-Shu hypothesis for many features we see in spiral galaxies. However it is impossible to explain spiral structure solely based om tidal interaction due to statistical unlikeliness that galaxies always interact on orbits needed for such spiral ams to form.

Other theories are based on spiral detonation waves or driving by a bar or oval distortions. The spiral detonation theorem uses the idea of self-propagating star formation driven by shock waves created by supernovae. A wave of star formation driven by this effect would eventually shear by differential rotation into the resemblance of a spiral arm. This theorem however doesn't explain the disk shape of the old disk population and needs quite fine-tuned star formation rates. Sanders & Huntley (1975), (1976) and Sanders & Huntley & Roberts (1977) show that a bar like distortion in the center of a galaxy can create a spiral pattern without the use of density-wave theorems. Even small distortions already create strong effects in the disk. However even placing a small non detectable oval distortion in the center of normal galaxies will probable not be enough to explain all spiral structure we see. Such distortions cannot explain the shape of the underlying old disk population nor the tightly woven spiral arms.

See table 8 for some numerical properties of spiral galaxies.

A.5 Irregulars

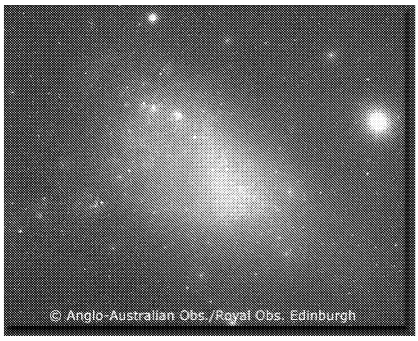

Figure 35: The Small Magellanic Cloud(SMC), type Irr

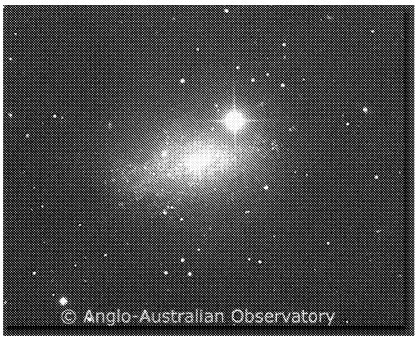

Figure 36: IC 5152, type Irr, including foreground star

Figure 37: Pictures of these galaxies are copyrighted to the AAO

Irregulars started out as refuge group which wasn't even depicted in Hubble's original tuning-fork diagram. Making up an only apparent two to three percent of all visible systems, Hubble decided they were end products of his galaxy evolution scheme or a peculiar object of one of the other three types of galaxies. However Hubble noticed that about half the irregulars resembled the appearance of the Magellanic Clouds. With the arrival of better telescopes it became apparent there are more irregular galaxies then Hubble suspected and there were clear similarities among the different systems in the group. de Vaucouleurs (1959) expanded and changed the most up to date Hubble diagram.
The Magellanic type irregulars, like the Large Magellanic Cloud(LMC), were moved to the spiral group and denoted Sm. Irregulars, like the Small Magellanic Cloud(SMC), were placed in the irregular group. The LMC type systems were moved to the spiral group since they posses spiral structure which however may not be immediately apparent. The SMC type systems are what remains of the Irregular group, these systems lack any form of apparent structure and are therefor best described as their name says; irregular.

Irregular systems contain an almost exclusive population of type I stars which makes them the bluest systems found in the universe. Irregulars make up the largest group of systems of the four discussed, in all probability dwarf type systems will be by far the most abundant but up till today not enough statistical data is available to support this claim for more then the local clusters. Irregulars are found in each type of universal environment in both high and low density regions they seem to be present, however there is a slight tendency towards lower density regions. See table 8 for some numerical

	Ellipticals	Lenticulars	Spirals	Irregulars
Mass ($M_\odot$)	10^5 to 10^{13}	10^9 to 10^{11}	10^9 to 10^{11}	10^8 to 10^{10}
Absolute magnitude	-9 to -23	-17 to -21	-15 to -21	-13 to -18
Luminosity ($L_\odot$)	10^5 to 10^{11}	10^8 to 10^{10}	10^8 to 10^{10}	10^7 to 10^9
M/L ($M_\odot/L_\odot$)	100	5 to 50	2 to 20	1
Radius (kpc)	$\sim$ 0.1 to 100	2 to 25	2 to 25	$\sim$ 0.1 to 5
Rotational velocities ($km\ s^{-1}$)	< 100	100 to 200	100 to 300	50 to 150
Population types	Type II, old Type I	Type II, old Type I	Type I (arms) and Type I and II (overall)	Type I and sometimes Type II
Dust presence	Almost none	Little to none	Some	Some
M_{HI}/M_T (%)	< 0.1	< 1	1 to 10	15 to 50
Color index ($B-V$)	+1.0	+0.8	+0.9 to +0.4	+0.3 to +0.4
Spectral type	K	G	K to A	A to F

Table 8: Characteristics of the four different main galaxy groups.

properties of irregular galaxies.

A.6 Lopsidedness

```
Webster's Revised Unabridged Dictionary (1913):

 Lopsided \Lop"sid'ed\, a. [Lop + side. Cf. Lobsided.]
    1. Leaning to one side because of some defect of structure;
       as, a lopsided ship. --Marryat.

    2. Unbalanced; poorly proportioned; full of idiosyncrasies.
       --J. S. Mill.


WordNet (r) 2.0 [wn]

 lopsided
      adj 1: out of proportion in shape [syn: ill-proportioned, one-sided]
      2: turned or twisted toward one side; "a...youth with a
         gorgeous red necktie all awry"- G.K.Chesterton; "his wig
         was, as the British say, skew-whiff" [syn: askew, awry(p),
         cockeyed, wonky, skew-whiff]
```

Maybe wonky galaxies would have been a better choice to denote the subject, some humour might have kept the subject in the spotlights. Since lopsidedness was mentioned first in the sixties the subject has only been touched ever so often and only in a few cases it has been researched in depth. The word however covers the load very well for the best examples of lopsidedness, especially in the visual part of the spectrum. In those cases a clear lobe is visual. In radio emission there are also some beautiful examples like M101.

The two examples show a clear deviation from symmetry and in different building blocks of a spiral galaxy, but why spiral systems? Spiral galaxies have one big advantage over both ellipticals and lenticulars, as the picture of M101 shows they don't lack neutral hydrogen gas(HI). Hydrogen gas is studied much more easily then the optical parts of galaxies. Radio astronomy allows for much better details to be seen when studying the effects of lopsidedness then ever is possible with optical telescopes, when comparing resolution to wavelength. Next to missing HI-gas, ellipticals and in lesser degree lenticulars suffer from the problem that they have no or almost no rotational velocities. This already touches on one of the parameters of a galaxy we study when we study lopsidedness, the velocity. The rotational velocities($ca.\ 200 - 300 kms^{-1}$) of spiral galaxies offer a high enough background to make a percentile deviation, the lopsidedness, more easily detectable when compared with the low dispersion velocities present in elliptical galaxies.

The other parameter studied next to the velocity or, kinematical part of the system is the distribution of matter in the system. For example when studying lopsidedness in the visual part of the spectrum this will be by studying the light distribution(almost exclusively emitted by stars), when studying the HI-gas it will be the HI-gas density.

As mentioned in the introduction research has shown that at least 50% of all spiral galaxies is lopsided in their HI distribution (Richter and Sancisi, 1994) and around 33% are lopsided in the visual part of the spectrum, mainly contributed to by red disk stars (Rix and Zaritsky, 1995).

Galaxies also appear to have a difference in strength in which lopsidedness appears depending on it occurring in the inner or outer regions of galaxies, it seems to appear much stronger towards the outer parts of a galaxy then it seems to appear on the inner parts. Physically the outer parts of galaxies are more easily disturbed then the inner parts, the larger mass density towards the center of galaxies has a dampening effect on disturbances. Next to dampening effects a spiral galaxy suffers from what astronomers call the winding effect, which in effect causes disturbances to disappear faster in the inner parts of a galaxy then in the outer parts.

Due to the high detail in which radio astronomers are able to study HI-gas in spiral galaxies and the greater strength in the outer parts of galaxies of perturbations this became the focal area for the study of lopsidedness.
Since galaxies can be disturbed in both density distribution and kinematics Richter & Sancisi (1994) in their paper study a large group of velocity profiles, see the figure on the front page for an example of a velocity profile(lower right corner).

The criteria they use for classification are peak flux differences ($\gtrsim 8\sigma$ or $\gtrsim 20\%$) between the horns in a profile, a total flux difference of ($\gtrsim 55:45\%$) between the low- and high-velocity halves and width differences ($\gtrsim 4$ velocity channels or $\gtrsim 50$ km s^{-1}) between the two horns. If a galaxy satisfies one of these conditions it is deemed lopsided. A galaxy that doesn't meet one of these conditions however doesn't have to be symmetric. A galaxy could for example fail to meet two of the three classification limits by a few percent. To include this Richter & Sancisi (1994) divided the group of lopsided galaxies into weak and strong examples, where the numbers given are a threshold between surely lopsided and most-likely lopsided, based on the quality if their data.

Velocity profiles are build up out of a combination of velocity data and data about the distribution of the HI-gas. This combination however allows for a cancellation of effects. To avoid missing cases of lopsidedness due to this effect one can study the velocity separately in a diagram next to a diagram of the HI-gas distribution.

The large occurrence percentage of lopsidedness hints at a structural effect as a cause for lopsidedness. Different paths have been taken by different researches over the last decades, to give a possible reason for lopsidedness. But for all of these researches one problem, that of winding, needed to be taken into account. Each spiral galaxy suffers from this so called winding effect as it rotates. The effect is most simply explained with a figure.

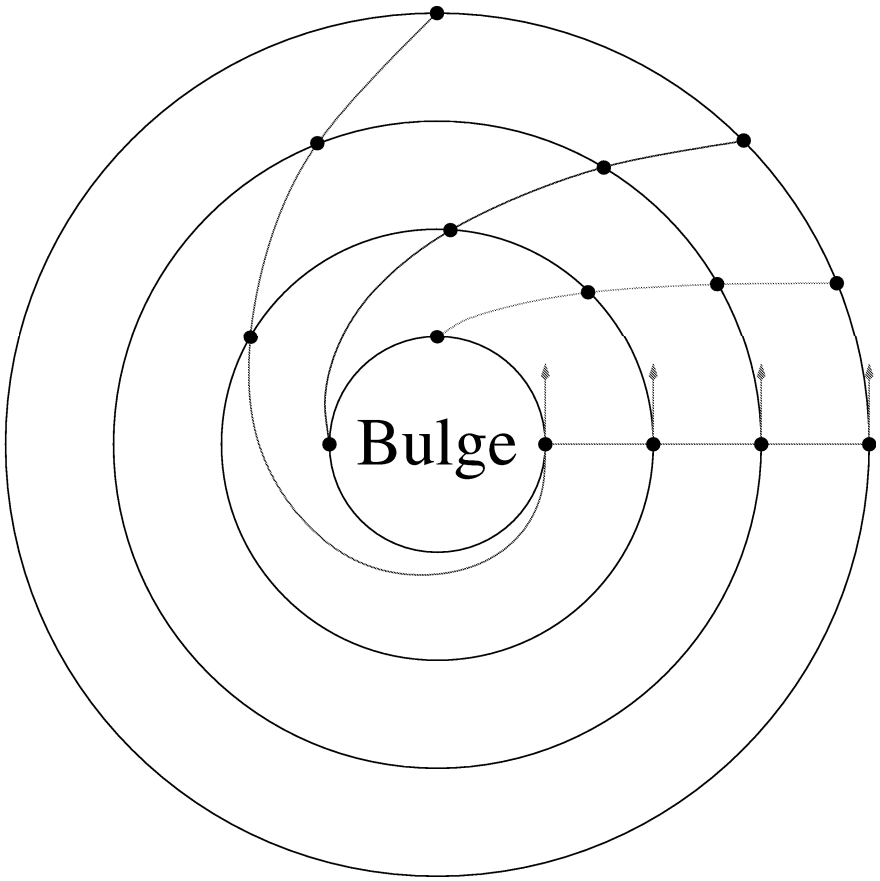

Figure 38: Winding problem, a spiral arm which starts out as a straight line(magenta) will slowly wind up. After one rotational period of the inner part of the arm the outer part of the arm will only have moved a quarter of its cycle, giving the arm a spiral appearance(red line).

In figure 38 it is clearly seen that a spiral arm will twist itself around the core of a galaxy as it rotates. This causes the stretching of the matter the arm was originally build out up of till it becomes so spread out the arm has practically dissolved itself. The same goes for a perturbation that is applied to the

original arm, this lopsidedness will slowly stretch out and disappear. Since rotational periods of galaxies are around several hundredth million years and galaxies are over or around ten times as old a perturbation that was present in the beginning is simply not noticeable anymore around our present day. Hence if we detect a significant number of lopsided galaxies they have to be recently perturbed in one way or another or the perturbation needs to be a part of the underlying physical system of a spiral galaxy.

In this research we will focus on the lopsidedness in the kinematics of galaxies with the help of the WHISP catalog. From this database a number of strongly lopsided galaxies will be taken and several parameters of those galaxies will be collected and compared with a larger control group. With this we hope to gain a better insight into strong lopsidedness, lopsidedness in general and a better grasp of what may or may not be able to induce this phenomena.

B Control sample

System	Type	D25(')	d25(')	ϵ	Inc..	m_B	M_B	L_B	D(Mpc)	M_{HI}	M_{tot}	ρ	Group	Comp.
UGC 79	Sc	1.38	1	0.28	44.73	15.50	-18.48	9.58	62.56	9.64	10.75			
UGC 655	Sm	2.69	2.69	0	0.00	14.82	-15.91	8.56	14.03	9.03				
UGC 1256	SBcd	6.92	2.57	0.63	70.66	10.50	-18.78	9.70	7.17	9.27	10.55	0.16	17 -5	
UGC 1281	Sdm	4.37	0.76	0.83	90.00	11.04	-16.83	8.92	3.75	8.45	9.36	0.13	17 +6	
UGC 1305	Sc	3.31	2.29	0.31	47.50	11.95	-20.97	10.58	38.45	9.55	11.33	0.26	52-15+14	
UGC 1313	SABc	2.29	1.41	0.38	53.50	13.27	-19.86	10.14	42.28	10.01	10.61			2
UGC 1437	SABc	2.4	1.74	0.28	44.73	12.53	-21.71	10.87	70.35	10.36	11.49			
UGC 1913	SABd	11.75	6.61	0.44	56.87	9.87	-19.98	10.18	9.34	9.75	10.80	0.48	17 -1	
UGC 2080	SABcd	5.37	4.9	0.09	24.64	11.44	-19.39	9.95	14.64	9.71	10.87	0.08	17 +1	
UGC 2459	Sdm	3.47	0.63	0.82	90.00				37.24	10.43	11.09	0.12	18 -1	
UGC 2800	Im	3.98	1.95	0.51	73.57				20.18	9.47	10.62	0.14	12-19	
UGC 2855	SABc	7.94	3.39	0.57	67.44	9.06	-22.50	11.19	20.53	10.00	11.51	0.14	12-19	
UGC 3273	Sm	3.55	1.32	0.63	90.00	12.61	-17.65	9.25	11.28	9.54	10.11	0.06	15 -0	
UGC 3371	Im	5.13	4.07	0.21	41.94	13.83	-17.08	9.02	15.2	9.26	10.46	0.11	12-11	
UGC 3574	Scd	3.55	3.24	0.09	24.64	14.29	-17.54	9.21	23.26	9.76	11.01	0.11	24 -2	
UGC 4165	SBd	2.95	2.75	0.07	21.33	12.11	-17.86	9.34	9.86	8.88	10.42	0.23	15+11+10	
UGC 4325	Sm	3.47	2	0.42	64.13	12.16	-17.83	9.32	9.96	8.86	9.87	0.25	15-11+10	
UGC 4701	Scd	1.7	0.85	0.5	61.58	14.71	-17.17	9.06	23.8	8.95	10.13			
UGC 5272	Im	2	0.76	0.62	90.00	13.82	-15.99	8.59	9.17	8.86	9.24	0.12	15 -0 +1	
UGC 5557	SABcd	7.94	7.59	0.05	17.55	10.30	-19.88	10.15	10.89	9.46	11.27	0.17	15 +7	
UGC 5685	Sbc	4.17	1.66	0.6	70.42	11.90	-19.72	10.08	21.07	9.62	11.19	0.38	21 -8	
UGC 5840	SABbc	7.41	7.08	0.05	17.74	10.32	-19.67	10.06	9.93	9.58	11.27	0.19	15 -0 +1	
UGC 6016	Im	2.04	1.29	0.37	58.60				24.43	9.38	9.91			1
UGC 6126	SBm	3.47	1.05	0.7	90.00	13.24	-17.15	9.05	11.95	9.54	10.16	0.26	15 -4 +1	
UGC 6128	SABc	1.66	1.48	0.11	27.58	12.82	-18.83	9.73	21.41	8.97	10.92	0.22	21 -7	
UGC 6225	SBcd	7.94	2.69	0.66	72.98	10.01	-20.60	10.43	13.23	9.85	11.02	0.15	12 -0+1	
UGC 6628	Sm	2.75	2.51	0.09	26.82	13.19	-17.71	9.27	15.1	9.12	9.67	1.21	12 -1	
UGC 6856	Sc	5.01	4.9	0.02	12.51	10.93	-19.87	10.14	14.48	9.63	11.20	1.24	12 -1	
UGC 6870	SBc	7.59	3.72	0.51	62.89	10.23	-21.08	10.63	18.31	9.41	11.43	1.20	12 -1	
UGC 6937	SBbc	7.08	4.57	0.35	51.66	10.34	-20.97	10.58	18.29	9.73	11.61	1.23	12 -1	
UGC 6964	Sm	3.72	0.78	0.79	90.00	11.98	-19.04	9.81	16.01	9.40	10.57	1.59	12 -1	
UGC 7047	Im	2.75	1.58	0.42	64.13	13.53	-15.49	8.39	6.38	8.55	9.01	0.47	14 -0	
UGC 7089	Sm	3.02	0.65	0.79	90.00	12.72	-18.01	9.40	14	9.23	9.94	1.09	12 -1	
UGC 7095	Sc	5.13	1.51	0.7	77.30	10.95	-20.39	10.35	18.53	9.62	11.15	1.02	12 -1	
UGC 7125	Sm	4.17	1.07	0.74	90.00	13.92	-17.34	9.13	17.9	9.90	10.18	0.29	12 -6 +1	
UGC 7232	Im(pec)	1.62	1.48	0.09	26.82	13.75	-15.13	8.24	5.96	8.26	9.27	0.37	14 -7	
UGC 7353	SABbc	16.6	6.31	0.62	71.79	8.39	-21.52	10.80	9.61	10.00	11.46	0.57	14 -4	
UGC 7399	SBd	2.19	1.62	0.26	42.82	13.09	-17.08	9.02	10.8	9.02	10.31	0.75	14 -4	
UGC 7592	IBm	5.62	3.72	0.34	55.67	9.64	-19.25	9.89	5.99	9.33	9.93	0.46	14 -7	

continued on next page

continued from last page													
UGC 7608	Im	3.55	3.24	0.09	26.82	13.53	-16.62	8.84	10.72	8.90	9.90	0.74	14 -4	
UGC 7774	Sd	2.82	0.43	0.85	90.00	13.53	-16.56	8.81	10.4	9.12	9.98	0.59	14 -4	
UGC 7853	SBm	4.37	3.39	0.22	43.91	11.15	-19.01	9.80	10.76	9.38	10.15	0.74	14 -4	Arp object
UGC 8303	I(AB)m	2.09	1.58	0.24	45.79	13.53	-17.54	9.21	16.34	8.96	9.72	0.30	43 -1	
UGC 8700	Sbc	3.55	0.98	0.72	80.87	12.39	-20.60	10.43	39.71	9.65	11.43	0.78	42 -1	
UGC 8709	SABb	4.9	1.15	0.77	90.00	11.36	-21.50	10.79	37.36	10.29	11.43	0.79	42 -1	
UGC 8711	Sb	3.89	0.81	0.79	90.00	12.16	-19.81	10.12	24.77	10.03	10.94	0.14	43 -0	
UGC 8837	IBm	3.98	1.2	0.7	90.00	12.74	-16.07	8.62	5.78	8.53	9.28	0.31	14 -9	
UGC 9242	Scd	4.37	0.28	0.94	90.00	12.05	-19.82	10.12	23.64	9.73	10.59	0.09	43 -0	
UGC 9431	Sc	2.95	0.45	0.85	90.00	12.68	-20.06	10.22	35.29	10.16	11.04	0.40	42 -3	
UGC 9753	Sbc	3.8	1.38	0.64	73.13	11.44	-19.43	9.96	14.93	9.21	10.64	0.21	44 -1	
UGC 10445	SBc	2.4	1.62	0.32	48.79	13.60	-17.51	9.20	16.71	9.24	10.18			
UGC 10470	SBbc	3.16	2.63	0.17	34.76	11.65	-20.21	10.28	23.53	9.93	10.98	0.15	44 -0 +5	Arp object 1
UGC 10502	Sc	2.29	1.86	0.19	36.49	13.26	-20.79	10.51	64.67	10.22	11.40			
UGC 10564	SBcd	2.4	1.17	0.51	62.39	14.19	-17.34	9.13	20.27	9.57	10.21	0.18	44 -6 +5	
UGC 10757	Sc	1.35	0.79	0.41	55.61	14.22	-17.37	9.14	20.83	9.23	10.26			
UGC 11218	Sc	4.79	2.34	0.51	62.89	10.90	-21.12	10.64	25.32	9.73	11.18	0.19	44 -8	
UGC 11283	SBdm	1.74	1.45	0.17	37.64	13.36	-19.14	9.85	31.61	9.71	10.80	0.07	70 -0	
UGC 11557	SABdm	2.63	2.09	0.21	41.94	13.35	-18.52	9.60	23.63	9.42	10.08	0.08	40 -0	
UGC 11864	SBd	2.82	2.04	0.28	44.28	14.14	-19.88	10.15	63.78	10.22	10.88			
UGC 12060	IBm	1.41	0.78	0.45	66.80	14.95	-15.93	8.56	15	9.15	9.52	0.29	65 -1	

C Lopsided sample

System	Type	D25(')	d25(')	ϵ	Incl.	m_B	M_B	L_B	D(Mpc)	M_{HI}	M_{tot}	ρ	Group	Comp.
UGC 731	Im	2.57	1.27	0.51	73.05	13.74	-15.78	8.50	8.00	8.78	9.59	0.13	17 -2	No
UGC 1249	Sm*	6.61	2.45	0.63	90.00	10.96	-18.43	9.56	7.54	9.28	9.92	0.27	17 -5	NGC 672
UGC 1501	SBd (P)	6.27	1.56	0.75	78.74	11.18	-17.60	9.23	5.70	9.03	9.51	0.15	17 +6	Possible
UGC 1888	SBc (P)	3.28	1.87	0.43	57.00	12.32	-19.38	9.94	21.90	9.42	10.78	0.06	52 -0	-
UGC 3137	Sbc*	2.60	0.60	0.77	87.65	14.38	-16.94	8.97	18.35	9.88	10.35	0.10	12+11	-
UGC 4278	SBd* (P)	6.60	0.78	0.88	90.00	11.99	-18.11	9.44	10.49	9.45	10.36	0.24	15+11+10	-
UGC 4499	Sdm*	2.34	1.94	0.17	38.21	14.21	-16.35	8.73	12.96	9.09	10.15	0.22	15-10	Possible
UGC 4806	Sc	2.92	0.78	0.73	79.70	11.79	-20.57	10.42	29.60	9.87	10.96	0.26	21-18	Yes
UGC 5251	SBbc*	5.89	1.40	0.76	86.10	11.36	-20.58	10.42	24.40	10.16	11.02	0.64	21-12	See remark
UGC 5316	SBd*	4.06	2.05	0.50	61.00	11.66	-19.78	10.10	19.40	9.92	10.63	0.23	12 -7	See remark
UGC 5414	Im	3.31	1.93	0.42	63.26	13.69	-16.31	8.72	9.99	8.77	9.66	0.15	15 +7	-
UGC 5446	Scd*	1.45	0.33	0.77	81.50	14.50	-16.78	8.90	18.00					Yes
UGC 5452	Sbc	2.40	0.55	0.77	90.00	13.31	-17.97	9.38	18.00	9.51	10.27			Yes
UGC 5459	Sc	3.30	0.67	0.80	90.00	11.98	-19.49	9.99	19.70	9.97	10.63	0.27	13 -1	-
UGC 5589	SBcd*	2.75	1.56	0.43	56.70	13.44	-18.17	9.46	21.00	9.56	10.42	0.22	13 -1	See remark
UGC 5721	S(B)d*	1.82	0.90	0.50	61.57	12.76	-16.37	8.74	6.70	8.85	9.51	0.19	15 -0 +1	See remark
UGC 5786	Sb(pec.)	2.75	2.37	0.14	31.20	10.93	-20.43	10.36	18.70	9.82	10.94	0.27	13 +1	See remark
UGC 5789	SBcd* (P)	5.96	3.45	0.42	56.00	11.37	-19.10	9.83	12.40	9.45	10.67	0.17	15 +7	Unlikely
UGC 5986	Sm	5.04	1.73	0.66	90.00	10.52	-19.20	9.87	8.80	9.65	10.41	0.19	15 +8 +7	Highly likely
UGC 6161	SBdm*	1.82	0.73	0.60	90.00	15.25	-15.31	8.32	12.93	9.02	9.53	0.16	15 -9	-
UGC 6251	Sm(dSph)	1.26	1.12	0.11	30.39	15.03	-15.57	8.42	13.18	8.68	9.25	0.59	12 -2 +1	-
UGC 6446	Sd* (P)	2.04	1.48	0.27	44.06	12.79	-18.16	9.46	15.50	9.38	10.09	0.56	12 -1	Possible
UGC 6667	Scd	2.18	0.27	0.88	90.00	13.49	-17.46	9.18	15.50	8.85	10.02	1.59	12 -1	-
UGC 6745	Sc (P)	4.01	1.03	0.74	80.76	11.06	-20.05	10.21	16.70	9.25	10.88	1.53	12 -1	Highly likely
UGC 6833	S(B)c	3.16	2.37	0.25	42.40	12.98	-18.36	9.53	18.50	9.44	10.48	0.38	12 +6 +1	No
UGC 6869	Sbc*	2.69	1.62	0.40	55.21	11.23	-19.72	10.08	15.50	9.36	10.62	1.61	12 -1	Yes
UGC 6955	SBm* (P)	4.18	2.08	0.50	72.70	12.68	-18.30	9.51	15.70	9.31	10.17	0.38	12 +6 +1	-
UGC 7030	SBbc* (P)	5.45	3.58	0.34	50.82	10.84	-20.11	10.24	15.50	9.37	10.98	1.06	12 -1	-
UGC 7075	S(B)c (P)	2.08	0.50	0.76	82.17	12.24	-18.71	9.68	15.50	9.13	10.39	1.31	12 -1	Possibly
UGC 7081	Sbc* (P)	4.40	1.65	0.63	72.20	10.75	-20.20	10.27	15.50	9.79	10.93	1.19	12 -1	Possibly
UGC 7090	S(B)c (P)	5.01	1.56	0.69	76.00	10.17	-19.70	10.07	9.40	9.08	10.66	0.40	14 -4	-
UGC 7151	S(B)cd* (P)	4.72	1.04	0.78	82.38	10.95	-17.22	9.08	4.30	8.41	9.56	0.42	14 -7	-
UGC 7222	Scd* (P)	3.30	0.52	0.84	90.00	12.12	-18.83	9.72	15.50	9.76	10.44	1.05	12 -1	Warped
UGC 7323	Sdm*	4.79	3.61	0.25	46.27	11.35	-18.18	9.46	8.05	8.84	10.07	0.68	14 -4	No
UGC 7524	Sm	12.02	7.60	0.37	58.49	10.79	-16.90	8.95	3.45	8.87	9.92	0.40	14 -7	-
UGC 7766	Sc	12.02	4.34	0.64	72.20	9.60	-20.33	10.33	9.70	9.76	10.84	1.01	14 -1	Yes
UGC 9119	Scd*(P)	3.49	1.13	0.68	74.00	12.15	-19.20	9.87	18.60	9.51	10.66	0.07	43 -0	No
UGC 10310	SBm	2.88	2.02	0.30	51.58	13.36	-17.60	9.23	15.56	9.07	9.82	0.08	44 -0	Possible
UGC 10359	SBc*	4.90	3.96	0.19	37.00	11.85	-19.50	9.99	18.60	9.94	11.02	0.12	44 -0 +1	Possible

continued on next page

continued from last page													
UGC 11300	Sd*	3.56	1.17	0.67	73.00	11.94	-18.42	9.56	11.80	9.12	1C.27	0.09	44 -0	No
UGC 11651	Scd	2.85	0.51	0.82	90.00	13.37	-18.53	9.60	24.00	9.74	1C.62	0.06	64 -0	-
UGC 11707	Sdm*	3.61	1.73	0.52	74.94	14.65	-16.36	8.73	15.90	9.54	1C.31	0.09	65 +5	No
UGC 11891	Im	4.07	3.14	0.23	44.30	13.63	-16.48	8.78	10.50	9.37	1C.26	0.07	65 -0	-
UGC 12632	Sm	2.50	1.40	0.44	65.81	12.96	-16.23	8.69	6.90	8.92	9.46	0.18	65 -4	No
UGC 12732	Sm	3.31	2.70	0.18	39.49	13.77	-16.83	8.93	13.20	9.43	1C.20	0.15	65 -3	Yes

D Improved control sample

System	Type	D25(')	d25(')	ϵ	Incl.	m_B	M_B	L_B	D(Mpc)	M_{HI}	M_{tot}	ρ
UGC 499	S0-a	24.08	17.93	0.26	46.07	14.01	-20.09	10.23	66.06	10.24	10.04	
UGC 528	SBb	8.29	8.27	0.00	4.03	10.81	-19.55	10.01	11.77	9.01	12.04	0.11
UGC 655	Sdm	10.38	10.38	0.00	0.00	14.53	-16.21	8.68	14.08	9.03		
UGC 1178	Scd	40.31	7.51	0.81	87.41	14.00	-20.52	10.40	80.29	10.43	11.25	
UGC 1281	Sdm	4.88	0.85	0.83	84.27	11.03	-16.85	8.93	3.75	8.47	9.37	0.13
UGC 1886	SBbc	54.09	34.37	0.36	52.58	14.46	-19.81	10.12	71.36	10.40	11.77	
UGC 2023	Im	6.93	6.67	0.04	17.57	13.50	-16.51	8.80	10.08	8.60	9.71	0.54
UGC 2034	IBm	8.28	6.85	0.17	38.10	13.29	-16.75	8.89	10.17	8.94	9.33	0.63
UGC 2080	SBcd	21.47	19.81	0.08	23.08	11.43	-19.40	9.95	14.69	9.76	10.90	0.08
UGC 2082	Scd	17.20	2.63	0.85	90.00	11.57	-18.63	9.65	10.96	9.49	10.31	0.18
UGC 2141	S0-a	10.96	5.02	0.54	72.18	12.87	-18.04	9.41	15.18	9.45	10.27	0.18
UGC 2193	Sc	7.27	5.21	0.28	45.42	11.57	-18.22	9.48	9.06	9.21	8.82	0.50
UGC 2487	E-S0	51.91	40.02	0.23	48.65	12.56	-21.74	10.89	72.20	9.81	11.75	
UGC 2503	SBb	44.19	25.96	0.41	57.03	11.03	-21.77	10.90	36.28	10.19	11.59	0.13
UGC 2800	Im	14.74	7.22	0.51	73.57		-31.53	14.81	20.27	9.48	10.42	0.14
UGC 2953	Sab	21.42	16.51	0.23	41.69	9.53	-21.50	10.79	16.07	9.84	11.53	0.08
UGC 3205	Sab	24.36	9.70	0.60	73.51	12.12	-21.47	10.78	52.23	10.10		
UGC 3354	Sab	25.62	8.08	0.68	81.77	13.31	-20.04	10.21	46.86	9.85	11.12	
UGC 3382	SBa	23.90	22.61	0.05	20.03	13.49	-20.64	10.45	67.24	9.72		
UGC 3384	Sm	4.23	3.50	0.17	38.32	16.62	-14.78	8.10	19.05	9.26	9.43	
UGC 3580	SBab	19.30	10.41	0.46	62.30	13.34	-18.22	9.48	20.55	9.65	10.60	0.08
UGC 3642	S0	29.61	23.30	0.21	44.48	13.14	-21.01	10.59	67.41	10.40	11.57	
UGC 3685	SBb	23.54	16.29	0.31	48.36	12.84	-19.45	9.97	28.71	10.01	10.12	0.20
UGC 3734	SBc	8.92	8.10	0.09	25.38	12.63	-18.41	9.56	16.13	9.10	10.61	0.06
UGC 3817	Im	4.39	2.26	0.48	70.54		-29.62	14.04	8.39	8.23	8.67	0.11
UGC 3965	SBab	18.53	17.37	0.06	21.29	14.62	-19.55	10.01	68.10	9.87	10.54	
UGC 3993	S0	19.11	16.38	0.14	36.12	14.48	-19.63	10.04	66.30	9.78	10.78	
UGC 4284	SBcd	17.67	8.83	0.50	61.58	11.60	-18.50	9.59	10.48	9.54	10.47	0.25
UGC 4305	Im	13.90	10.35	0.26	47.24	10.73	-18.09	9.43	5.80	9.40	9.59	0.29
UGC 4458	Sa	36.66	32.52	0.11	29.25	13.05	-21.13	10.64	68.62	10.06	11.57	
UGC 4543	Sdm	19.51	13.47	0.31	52.75	15.22	-17.19	9.07	30.38	9.80	10.18	0.15
UGC 4605	SBab	27.40	5.03	0.82	90.00	11.66	-20.09	10.23	22.33	9.89	11.17	0.26
UGC 4806	Sc	31.10	8.16	0.74	79.66	11.79	-20.56	10.41	29.52	9.88	11.05	0.26
UGC 4838	SBc	33.51	21.14	0.37	52.35	11.96	-21.05	10.61	39.95	10.12	10.85	0.10
UGC 5079	SBbc	32.60	14.27	0.56	67.45	8.86	-20.90	10.55	8.94	9.73	11.21	0.12
UGC 5272	IBm	5.39	2.06	0.62	90.00	13.82	-16.00	8.59	9.18	8.86	9.24	0.12
UGC 5446	Scd	9.03	2.09	0.77	81.69	14.49	-17.19	9.07	21.67	15.00		
UGC 5557	SBcd	24.93	23.80	0.05	17.55	10.30	-19.89	10.15	10.91	9.51	11.26	0.17
UGC 5582	SBbc	31.58	19.38	0.39	54.23	12.21	-21.19	10.67	47.94	10.08	11.18	

continued on next page

continued from last page												
UGC 5685	Sbc	26.51	10.46	0.61	70.81	11.90	-19.73	10.08	21.17	9.63	11.21	0.38
UGC 5840	SBbc	20.78	19.89	0.04	17.27	10.31	-19.68	10.06	9.95	9.63	11.28	0.19
UGC 5960	S0	6.01	2.63	0.56	90.00	12.65	-17.62	9.24	11.33	9.00	9.78	
UGC 6001	Sab	4.36	2.95	0.32	50.79	14.38	-17.77	9.30	26.92	8.71	9.80	0.21
UGC 6128	SBc	10.27	9.13	0.11	27.85	12.82	-18.84	9.73	21.52	8.98	10.91	0.22
UGC 6225	SBcd	31.58	10.58	0.67	73.19	10.00	-20.61	10.44	13.27	9.90	11.03	0.15
UGC 6446	Sd	10.05	7.05	0.30	46.18	13.47	-17.02	9.00	12.52	9.21	10.10	0.56
UGC 6456		0.71	0.43	0.39	60.85	15.72	-11.39	6.75	2.65	7.42	7.95	0.46
UGC 6786	S0	24.92	12.72	0.49	70.10	12.28	-19.94	10.17	27.72	9.50	11.18	0.13
UGC 6787	Sab	21.75	14.07	0.35	52.83	11.28	-20.26	10.29	20.26	9.53	11.37	0.56
UGC 6833	SBc	14.40	10.82	0.25	42.23	12.97	-18.02	9.40	15.76	9.32	10.41	0.38
UGC 6937	SBbc	37.39	23.98	0.36	52.11	10.34	-20.99	10.59	18.37	9.78	11.60	1.23
UGC 7075	SBc	10.06	2.73	0.73	79.15	12.12	-18.61	9.64	13.99	9.04	10.42	1.31
UGC 7166	SBab	29.95	23.62	0.21	39.97	10.31	-20.85	10.53	17.01	9.58	10.64	0.36
UGC 7183	SBb	27.83	4.87	0.83	90.00	10.98	-19.81	10.12	14.38	10.05	11.15	1.19
UGC 7204	SBd	21.14	4.34	0.79	82.27	12.47	-18.81	9.72	18.09	9.83	10.20	0.98
UGC 7278	IBm	17.80	14.10	0.21	42.14	9.88	-19.30	9.91	6.83	9.61	9.93	0.40
UGC 7483	SBc	17.57	7.05	0.60	69.29	13.32	-18.21	9.48	20.28	9.37	10.41	1.13
UGC 7916	Im	7.96	5.84	0.27	48.29	14.67	-15.61	8.44	11.35	8.82	9.36	0.53
UGC 8246	SBcd	14.16	2.63	0.81	88.31	13.38	-17.38	9.14	14.20	9.27	10.04	0.30
UGC 8403	SBcd	18.54	12.34	0.33	49.44	12.38	-18.76	9.70	16.92	9.52	10.66	0.28
UGC 8490	Sm	9.18	5.92	0.36	57.30	11.30	-17.83	9.33	6.72	9.07	9.80	0.29
UGC 8508	Im	2.29	1.39	0.39	60.71	14.33	-13.98	7.78	4.60	7.91	8.53	0.34
UGC 8699	SBab	21.64	6.67	0.69	83.90	13.26	-19.71	10.08	39.14	9.56	10.95	
UGC 8709	SBc	56.74	13.18	0.77	84.10	11.35	-21.53	10.80	37.69	10.32	11.46	0.79
UGC 8711	SBbc	29.19	6.13	0.79	90.00	12.15	-19.83	10.12	24.92	10.04	10.96	0.14
UGC 8863	SBa	29.87	14.07	0.53	68.87	11.99	-20.33	10.32	29.08	9.34	11.16	0.19
UGC 9133	Sab	51.42	29.38	0.43	58.96	12.36	-21.47	10.78	58.26	10.02	11.63	
UGC 9211	Im	4.72	2.54	0.46	68.00	16.77	-13.86	7.74	13.35	9.04	9.27	0.08
UGC 9242	Sd	33.48	2.12	0.94	90.00	12.05	-19.83	10.12	23.77	9.76	10.64	0.09
UGC 9431	Scd	32.36	4.88	0.85	90.00	12.66	-20.09	10.23	35.59	10.18	11.06	0.40
UGC 9644	SBa	34.04	31.47	0.08	23.74	15.70	-19.25	9.89	98.00	9.74	11.01	
UGC 9648	Sc	25.39	13.23	0.48	60.62	13.94	-19.64	10.05	52.10	9.56	9.69	
UGC 9753	Sbc	17.24	6.22	0.64	73.59	11.44	-19.44	9.97	14.99	9.21	10.65	0.21
UGC 9805	Sb	48.19	20.99	0.56	68.69	12.20	-21.35	10.73	51.20	10.10	11.87	
UGC 10470	SBbc	21.12	17.57	0.17	34.82	11.65	-20.22	10.28	23.66	9.94	10.97	0.15
UGC 10564	SBd	14.28	7.08	0.50	61.67	14.16	-17.38	9.15	20.37	9.58	10.22	0.18
UGC 10897	SBc	16.05	14.37	0.10	27.03	12.18	-19.64	10.05	23.11	9.47	10.63	0.23
UGC 11670	S0-a	17.81	5.65	0.68	90.00	11.15	-19.54	10.01	13.71	9.37	10.80	0.08
UGC 11909	Sc	13.62	3.21	0.76	83.39	12.83	-18.56	9.62	18.98	9.50	10.37	0.06
continued on next page												

continued from last page											
UGC 12043	S0-a	8.36	2.90	0.65	90.00	13.93	-17.17	9.06	16.53	9.18	
UGC 12060	IBm	5.81	3.19	0.45	66.80	14.93	-15.95	8.57	15.05	9.16	9.50	0.29

E Improved lopsided sample

System	Type	D25(')	d25(')	ϵ	Incl.	m_B	M_B	L_B	D(Mpc)	M_{HI}	M_{tot}	ρ
UGC 89	SBab	35.96	27.66	0.23	42.25	14.29	-19.84	10.13	66.69	9.91	11.60	
UGC 232	SBa	22.98	16.34	0.29	48.11	14.29	-19.97	10.18	71.06	9.85	-	
UGC 508	SBab	58.36	56.90	0.03	13.46	12.19	-21.98	10.98	68.14	10.15	12.87	
UGC 623	Sa	22.74	9.03	0.60	76.36	14.35	-19.89	10.15	70.49	9.32	11.04	
UGC 624	Sab	36.60	13.11	0.64	77.12	12.79	-21.42	10.76	69.78	10.14	11.52	
UGC 625	SBbc	40.79	11.68	0.71	79.96	12.13	-20.88	10.54	39.97	10.21	11.16	0.11
UGC 690	SBcd	50.11	36.89	0.26	43.50	13.58	-21.09	10.63	85.94	10.14	11.54	
UGC 731	Im	7.49	6.87	0.08	26.16	14.12	-16.24	8.69	11.80	9.14	10.36	0.13
UGC 798	SBa	24.18	14.50	0.40	57.92	14.59	-19.67	10.06	71.40	9.87	-	
UGC 1249	SBm	11.86	4.57	0.61	90.00	10.96	-17.97	9.38	6.10	9.17	9.83	0.15
UGC 1305	Sbc	35.69	24.86	0.30	47.51	11.95	-21.00	10.59	38.80	9.58	11.32	0.26
UGC 1317	SBc	56.99	18.36	0.68	75.26	11.63	-21.65	10.85	45.30	10.57	11.58	
UGC 1501	SBdm	6.91	1.73	0.75	78.06	11.12	-16.91	8.95	4.04	8.77	9.44	0.15
UGC 1541	SBa	34.01	28.75	0.15	34.46	13.48	-21.10	10.63	82.39	10.11	11.78	
UGC 1550	Sc	74.00	15.82	0.79	85.87	12.71	-21.92	10.96	84.05	10.49	11.64	
UGC 1856	Sd	45.04	6.33	0.86	90.00	13.29	-20.93	10.56	69.96	10.57	10.97	
UGC 1993	Sb	70.72	15.54	0.78	90.00	13.76	-21.57	10.82	116.36	10.66	-	
UGC 2045	Sab	21.95	10.78	0.51	65.55	11.43	-20.39	10.35	23.16	9.13	10.95	0.06
UGC 2183	Sa	15.67	8.79	0.44	61.23	12.00	-19.82	10.12	23.14	9.63	-	
UGC 2459	Sdm	27.01	4.93	0.82	83.34		-32.87	15.34	37.57	10.44	10.95	0.12
UGC 2855	SBc	24.85	10.67	0.57	67.02	9.03	-22.54	11.21	20.63	10.03	11.23	0.14
UGC 2916	Sab	33.93	32.25	0.05	18.93	13.33	-20.84	10.53	68.05	10.45	-	
UGC 3013	SBb	46.71	26.27	0.44	58.69	11.43	-21.52	10.80	38.79	10.14	11.32	0.20
UGC 3137	Sbc	18.43	2.81	0.85	90.00	13.25	-18.00	9.39	17.82	9.87	10.47	0.10
UGC 3273	SBm	8.27	3.09	0.63	90.00	12.23	-18.04	9.41	11.32	9.55	9.97	0.06
UGC 3334	SBc	73.14	50.72	0.31	47.36	10.92	-22.95	11.37	59.49	10.83	12.27	
UGC 3371	Im	19.96	15.93	0.20	41.53	13.83	-17.09	9.03	15.26	9.30	10.41	0.11
UGC 3422	SBb	34.68	20.47	0.41	56.59	13.37	-20.57	10.42	61.42	10.18	11.41	
UGC 3546	SBa	24.96	16.57	0.34	52.49	12.16	-20.17	10.26	29.28	9.37	11.18	0.19
UGC 3574	Scd	23.32	21.51	0.08	23.10	14.27	-17.58	9.22	23.39	9.79	11.05	0.11
UGC 3711	IBm	4.90	3.70	0.24	46.16	12.14	-17.45	9.17	8.27	8.81	9.87	0.10
UGC 3740	SBc	30.16	26.03	0.14	31.00	11.52	-21.40	10.75	38.35	9.87	11.04	0.13
UGC 3851	IBm	9.77	3.34	0.66	90.00	10.82	-17.60	9.23	4.85	9.52	9.57	0.40
UGC 3909	SBcd	11.80	2.78	0.76	81.44	13.88	-17.28	9.11	17.10	9.12	-	
UGC 3992	Sab	0.00	0.00	0.14	32.55	-	-	-	-	-	-	
UGC 4165	SBd	8.25	7.72	0.06	21.00	12.10	-17.87	9.34	9.88	8.88	10.42	0.23
UGC 4173	Im	6.83	2.55	0.63	90.00	16.39	-14.65	8.05	16.14	9.60	9.11	0.10
UGC 4256	SBc	43.06	35.33	0.18	35.66	12.71	-21.71	10.88	76.62	10.24	11.20	
UGC 4278	SBd	12.31	1.54	0.87	90.00	11.57	-18.50	9.59	10.29	9.45	10.14	0.24

continued on next page

continued from last page												
UGC 4325	SBm	9.91	5.66	0.43	64.53	12.16	-17.84	9.33	9.98	8.88	9.86	0.25
UGC 4499	SBdm	8.62	4.83	0.44	56.84	14.18	-16.31	8.72	12.58	9.07	9.88	0.22
UGC 4666	S0	22.53	11.11	0.51	72.94	11.77	-19.21	9.88	15.67	9.21	10.91	0.13
UGC 4701	Sd	11.77	5.93	0.50	61.05	14.68	-17.21	9.08	23.93	8.95	10.14	
UGC 5251	SBbc	39.25	9.03	0.77	86.00	11.35	-20.46	10.37	23.02	10.12	10.99	0.64
UGC 5316	SBd	22.47	9.28	0.59	67.40	11.65	-19.73	10.08	18.87	9.91	10.58	0.23
UGC 5414	IBm	10.63	7.21	0.32	54.00	13.41	-16.82	8.92	11.09	8.88	9.79	0.15
UGC 5452	Sbc	14.82	2.67	0.82	90.00	13.28	-18.34	9.53	21.09	9.65	10.34	
UGC 5459	SBc	24.93	4.29	0.83	90.00	11.89	-19.49	9.99	18.92	9.96	10.75	0.27
UGC 5532	Sbc	54.47	47.01	0.14	31.28	11.15	-22.07	11.02	44.00	10.18	11.97	0.14
UGC 5589	SBcd	15.89	9.04	0.43	56.67	13.41	-18.07	9.42	19.79	9.51	10.40	0.22
UGC 5717	SBbc	17.34	8.81	0.49	62.20	12.17	-20.03	10.20	27.56	9.84	10.60	0.20
UGC 5721	SBd	4.99	2.52	0.50	60.90	12.75	-17.11	9.03	9.37	9.15	9.76	0.19
UGC 5786	SBbc	13.82	13.14	0.05	18.59	10.93	-20.25	10.29	17.25	9.76	11.33	0.27
UGC 5789	SBcd	22.36	11.98	0.46	59.19	11.33	-19.26	9.90	13.15	9.51	10.65	0.17
UGC 5829	IBm	15.00	7.05	0.53	76.20	13.04	-17.19	9.07	11.10	9.31	9.60	0.20
UGC 5986	SBm	22.25	5.56	0.75	90.00	10.52	-19.72	10.08	11.13	9.89	10.65	0.19
UGC 5997	Sbc	19.18	8.00	0.58	68.80	11.81	-19.89	10.15	21.83	9.72	10.76	0.24
UGC 6126	SBdm	12.20	3.72	0.70	90.00	13.23	-17.16	9.06	11.99	9.56	10.17	0.26
UGC 6161	SBdm	7.12	3.17	0.56	64.86	15.26	-15.41	8.36	13.61	9.07	9.64	0.16
UGC 6263	SBb	23.13	14.03	0.39	55.21	13.04	-19.59	10.03	33.53	9.84	11.10	0.15
UGC 6283	Sa	13.64	3.54	0.74	90.00	13.38	-17.19	9.07	12.97	9.65	10.26	0.14
UGC 6537	SBc	26.94	18.05	0.33	49.23	10.52	-20.40	10.35	15.30	9.81	11.06	1.21
UGC 6628	SBm	11.89	10.87	0.09	26.49	13.19	-17.72	9.28	15.16	9.14	9.67	1.21
UGC 6713	SBm	6.46	5.01	0.23	44.11	14.97	-16.06	8.62	16.02	8.90	9.68	1.55
UGC 6733	SBc	11.04	4.80	0.57	66.80	13.69	-17.82	9.32	19.96	9.02	10.05	0.52
UGC 6778	SBc	20.11	10.90	0.46	59.20	10.83	-20.33	10.32	17.05	9.75	10.87	1.65
UGC 6816	IBm	7.00	6.22	0.11	30.22	14.05	-17.00	8.99	16.19	8.92	10.17	0.91
UGC 6856	Sc	21.00	20.47	0.03	13.10	10.93	-19.88	10.15	14.53	9.65	11.16	1.24
UGC 6869	Sbc	11.34	6.63	0.42	56.37	11.22	-19.60	10.03	14.59	9.32	10.57	1.61
UGC 6930	SBd	13.79	11.41	0.17	34.60	12.64	-18.14	9.45	14.35	9.31	10.34	1.56
UGC 6964	SBd	18.19	3.85	0.79	81.84	11.98	-19.05	9.81	16.08	9.42	10.61	1.59
UGC 7030	SBbc	19.39	17.08	0.12	29.03	10.75	-19.83	10.12	13.05	9.25	11.28	1.06
UGC 7047	Im	5.12	2.94	0.43	64.26	13.51	-15.52	8.40	6.39	8.56	9.01	0.47
UGC 7081	SBc	24.57	9.36	0.62	71.09	10.39	-20.36	10.34	14.12	9.73	11.03	1.19
UGC 7089	Sdm	12.97	2.77	0.79	80.73	12.72	-18.02	9.40	14.04	9.25	9.97	1.09
UGC 7090	SBc	20.86	5.26	0.75	80.74	10.40	-19.84	10.13	11.18	9.26	10.83	0.40
UGC 7151	SBcd	12.10	2.57	0.79	83.66	10.95	-18.26	9.50	6.97	8.84	9.97	0.42
UGC 7222	Scd	24.09	3.33	0.86	90.00	11.43	-19.63	10.05	16.33	9.82	10.65	1.05
UGC 7256	E-SB0	18.08	12.83	0.29	56.57	11.81	-19.47	9.98	18.05	9.29	10.72	0.94
continued on next page												

continued from last page												
UGC 7261	SBdm	15.10	13.15	0.13	32.75	13.60	-17.10	9.03	13.81	9.22	10.17	0.31
UGC 7321	Sd	12.34	0.81	0.93	90.00	11.95	-17.50	9.19	7.74	9.10	10.26	0.28
UGC 7323	SBdm	14.69	10.21	0.30	46.58	11.34	-18.77	9.70	10.53	9.11	10.18	0.68
UGC 7353	SBbc	47.13	18.04	0.62	71.83	8.38	-21.54	10.81	9.63	10.16	11.46	0.57
UGC 7399	SBd	6.83	5.08	0.26	42.46	13.08	-17.09	9.03	10.82	9.03	10.32	0.75
UGC 7524	SBm	25.25	12.98	0.49	70.68	10.79	-18.48	9.58	7.14	9.59	10.15	0.40
UGC 7559	IBm	6.11	3.98	0.35	56.56	13.74	-15.11	8.23	5.88	8.34	9.14	0.37
UGC 7603	SBd	8.21	2.64	0.68	73.68	12.83	-17.41	9.15	11.13	9.02	9.67	0.17
UGC 7608	Im	10.90	10.06	0.08	25.12	13.53	-16.62	8.84	10.74	8.94	9.95	0.74
UGC 7651	SBd	20.74	8.89	0.57	66.25	9.87	-20.39	10.35	11.27	9.99	10.62	0.77
UGC 7690	Im	5.06	4.47	0.11	30.80	13.12	-17.03	9.01	10.74	8.76	9.71	0.74
UGC 7766	SBcd	49.31	17.25	0.65	72.05	9.59	-21.13	10.64	13.94	10.08	11.01	1.01
UGC 7774	Sd	9.12	1.39	0.85	90.00	13.51	-16.58	8.82	10.42	9.13	10.01	0.59
UGC 7831	SBc	10.15	4.17	0.59	68.55	10.14	-18.70	9.67	5.86	8.68	10.05	0.37
UGC 7853	SBdm	13.53	10.43	0.23	44.49	11.15	-19.02	9.80	10.78	9.42	10.14	0.74
UGC 7866	IBm	8.12	6.26	0.23	44.49	13.43	-16.09	8.63	8.02	8.55	9.21	0.35
UGC 7971	Sm	6.62	6.13	0.08	24.76	13.32	-16.71	8.88	10.15	8.58	9.74	0.55
UGC 8146	Sd	12.30	2.11	0.83	87.11	13.14	-17.48	9.18	13.31	9.25	10.01	0.10
UGC 8303	IBm	9.88	7.51	0.24	45.61	13.53	-17.55	9.21	16.41	8.97	9.73	0.30
UGC 8396	SBd	8.23	2.42	0.71	75.55	13.32	-17.77	9.30	16.55	9.06	9.88	0.29
UGC 8550	SBd	7.56	1.63	0.78	81.49	13.46	-16.24	8.69	8.69	9.02	9.69	0.33
UGC 8700	Sbc	43.03	11.77	0.73	81.33	12.38	-20.63	10.44	40.09	9.67	11.45	0.78
UGC 8837	IBm	6.86	2.05	0.70	90.00	12.73	-16.08	8.62	5.79	8.55	9.29	0.31
UGC 8900	Sb	39.19	20.62	0.47	61.49	11.63	-21.99	10.99	52.90	10.27	11.76	
UGC 9366	Sc	37.68	17.18	0.54	65.67	11.16	-21.49	10.79	33.83	9.93	11.48	0.43
UGC 9649	SBb	9.79	5.03	0.49	62.50	13.52	-16.61	8.84	10.60	9.02	9.98	0.09
UGC 9797	SBb	58.20	35.72	0.39	54.53	12.67	-20.93	10.56	52.38	10.52	11.51	
UGC 9858	SBbc	51.05	9.89	0.81	90.00	12.40	-20.66	10.46	40.95	10.58	11.34	0.29
UGC 10310	SBm	11.62	8.96	0.23	44.49	13.36	-17.37	9.14	13.98	8.99	9.88	0.08
UGC 10359	SBcd	24.35	19.65	0.19	36.92	11.85	-19.32	9.92	17.13	9.90	10.98	0.12
UGC 10713	Sb	10.53	1.95	0.81	90.00	12.44	-19.02	9.80	19.58	9.45	10.31	
UGC 10791	SBm	12.00	10.74	0.10	29.34	14.86	-16.97	8.98	23.20	8.76	10.55	
UGC 11124	SBcd	19.26	17.41	0.10	25.81	13.26	-18.84	9.73	26.30	9.56	10.88	0.08
UGC 11218	Sc	34.49	17.09	0.50	62.32	10.90	-21.13	10.64	25.47	9.74	11.18	0.19
UGC 11269	SBab	27.69	15.43	0.44	60.22	12.93	-20.14	10.25	41.07	10.03	11.24	0.06
UGC 11300	SBd	12.83	3.77	0.71	75.85	11.93	-18.32	9.52	11.18	9.08	10.28	0.09
UGC 11466	Sc	7.43	4.45	0.40	54.78	12.62	-18.30	9.51	15.24	9.40	10.24	
UGC 11707	Sdm	11.20	6.24	0.44	57.02	14.64	-16.29	8.71	15.29	9.51	10.25	0.09
UGC 11852	SBa	26.62	16.68	0.37	55.61	14.41	-20.26	10.30	85.81	10.36	-	
UGC 11861	SBdm	19.45	10.71	0.45	57.50	12.15	-19.85	10.13	25.13	9.96	10.74	0.07
continued on next page												

continued from last page												
UGC 11864	SBdm	41.11	29.58	0.28	44.56	13.85	-20.21	10.28	64.75	10.24	10.77	
UGC 11891	Im	11.37	8.79	0.23	44.30	13.31	-16.61	8.84	9.64	9.32	10.21	0.07
UGC 11914	Sab	16.97	14.38	0.15	33.65	10.56	-20.45	10.37	15.92	8.95	11.23	0.15
UGC 11951	SBa	10.12	3.50	0.65	82.16	11.89	-19.46	9.97	18.60	9.29	10.12	
UGC 12082	SBm	11.18	9.62	0.14	34.02	13.59	-17.12	9.04	13.85	9.15	9.82	0.31
UGC 12212	Sm	8.32	5.24	0.37	58.74		-30.85	14.53	14.81	8.91	9.65	0.23
UGC 12276	SBa	31.80	25.50	0.20	39.20	14.01	-20.59	10.43	83.32	9.80	10.57	
UGC 12554	SBc	22.70	4.40	0.81	90.00	10.13	-19.36	9.93	7.87	10.10	10.65	0.18
UGC 12632	SBm	11.18	9.23	0.17	38.32	12.06	-17.61	9.24	8.60	9.15	10.14	0.18
UGC 12693	SBcd	35.48	4.68	0.87	90.00	14.32	-19.99	10.19	72.82	10.52	10.76	
UGC 12732	SBm	11.88	10.42	0.12	31.91	13.59	-16.87	8.94	12.33	9.39	10.33	0.15
UGC 12754	SBcd	14.74	10.01	0.32	48.27	11.46	-19.00	9.79	12.35	9.25	10.53	0.14

F Ellipticity-Inclination correlation function

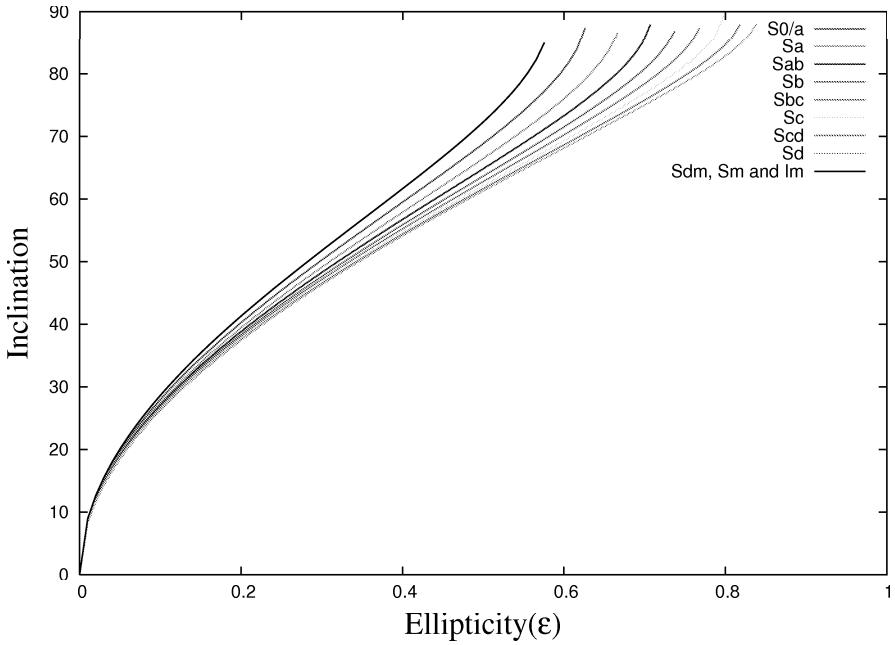

Figure 39: Correlation between the inclination and the ellipticity for a given morphological type

References

Arp, H.: 1966, *ApJS* **14**, 1
Baldwin, J. E., Lynden-Bell, D., and Sancisi, R.: 1980, *MNRAS* **193**, 313
Broeils, A. H.: 1992, *Ph.D. Thesis*
de Vaucouleurs, G.: 1959, *Handbuch der Physik*, Berlin: Springer, 1959, vol 53, p. 275
Haynes, M. P., van Zee, L., Hogg, D. E., Roberts, M. S., and Maddalena, R. J.: 1998, *AJ* **115**, 62
Hubble, E. P.: 1936, *Yale University Press*
Huntley, J. M., Sanders, R. H., and Roberts, W. W.: 1977, *BAAS* **9**, 639
Jog, C. J.: 1997, *ApJ* **488**, 642
Jog, C. J.: 1999, *ApJ* **522**, 661
Kornreich, D. A., Haynes, M. P., Jore, K. P., and Lovelace, R. V. E.: 2001, *AJ* **121**, 1358
Kornreich, D. A., Haynes, M. P., Lovelace, R. V. E., and van Zee, L.: 2000, *AJ* **120**, 139
Levine, S. E. and Sparke, L. S.: 1998, *ApJ* **496**, L13
Lin, C. C. and Shu, F. H.: 1964, *ApJ* **140**, 646
Lin, C. C. and Shu, F. H.: 1966, *Proceedings of the National Academy of Science* **55**, 229
Matthews, L. D., van Driel, W., and Gallagher, J. S.: 1998a, *AJ* **116**, 2196
Matthews, L. D., van Driel, W., and Gallagher, J. S.: 1998b, *AJ* **116**, 1169
Nilson, P.: 1973, *Nova Acta Regiae Soc. Sci. Upsaliensis Ser. V*
Noordermeer, E., Sparke, L. S., and Levine, S. E.: 2001, *MNRAS* **328**, 1064
Rhee, M.-H.: 1996, *Ph.D. Thesis*
Richter, O.-G. and Sancisi, R.: 1994, *A&A* **290**, L9
Rix, H. and Zaritsky, D.: 1995, *ApJ* **447**, 82
Roberts, M. S. and Haynes, M. P.: 1994, *ARA&A* **32**, 115
Rudnick, G. and Rix, H.: 1998, *AJ* **116**, 1163
Sancisi, R. and Allen, R. J.: 1979, *A&A* **74**, 73
Sandage, A.: 1961, *The Hubble atlas of galaxies*, Washington: Carnegie Institution, 1961
Sanders, R. H. and Huntley, J. M.: 1975, *BAAS* **7**, 513
Sanders, R. H. and Huntley, J. M.: 1976, *ApJ* **209**, 53
Schoenmakers, R. H. M., Franx, M., and de Zeeuw, P. T.: 1997, *MNRAS* **292**, 349
Sellwood, J. A. and Carlberg, R. G.: 1984, *ApJ* **282**, 61
Swaters, R. A.: 1999, *Ph.D. Thesis*
Swaters, R. A., Schoenmakers, R. H. M., Sancisi, R., and van Albada, T. S.: 1999, *MNRAS* **304**, 330
Toomre, A.: 1981, in *Structure and Evolution of Normal Galaxies*, pp 111–136
Toomre, A. and Toomre, J.: 1972, *BAAS* **4**, 214
Tully, R. B.: 1988, *Nearby galaxies catalog*, Cambridge and New York, Cambridge University Press, 1988, 221 p.
van der Hulst, J. M., van Albada, T. S., and Sancisi, R.: 2001, in

Astronomical Society of the Pacific Conference Series, p. 451
Verheijen, M. A. W.: 1997, *Ph.D. Thesis*
Vesperini, E. and Weinberg, M. D.: 2000, *ApJ* **534**, 598
Walker, I. R., Mihos, J. C., and Hernquist, L.: 1996, *ApJ* **460**, 121
Weinberg, M. D.: 1991, *ApJ* **368**, 66
Weinberg, M. D.: 1994, *ApJ* **421**, 481
Zaritsky, D. and Rix, H.: 1997, *ApJ* **477**, 118